PBTK-TD model of the phagocytosis activity in three-spined stickleback exposed to BPA

Corentin Mit, Anne Bado-Nilles, Cyril Turiès, Gaëlle Daniele, Barbara Giroud, Rémy Beaudouin

PBTK-TD model of the phagocytosis activity in three-spined stickleback exposed to BPA

Corentin Mit [1,2], Anne Bado-Nilles [2], Cyril Turiès [2], Gaëlle Daniele [3], Barbara Giroud [3] and Rémy Beaudouin[1]*

[1] Experimental Toxicology and Modeling Unit, INERIS, UMR-I 02 SEBIO, Verneuil en Halatte, 65550, France. Tel: +33344618238

[2] Ecotoxicology of substances and fields Unit, INERIS, UMR-I 02 SEBIO, Verneuil en Halatte, 65550, France

[3] Univ Lyon, CNRS, Université Claude Bernard Lyon 1, Institut des Sciences Analytiques, UMR 5280, 5 rue de la Doua, F-69100, Villeurbanne, France

*Corresponding author, e-mail: remy.beaudouin@ineris.fr

Abstract

Due to the high production volume and persistence in the environment of bisphenol A (BPA) and its substitutes, realistic exposure scenarii were proposed in some species to better understand the relationship between external and internal concentrations. For example, a recent PBTK model has been developed and adapted to BPA ADME (Absorption, Distribution, Metabolization, and Excretion) processes in three-spined stickleback. These substances have an impact on organism physiology including reproductive and immune functions. In this context, physiologically-based toxicokinetic models coupled with toxicodynamics (PBTK-TD) have proven to be valuable tools to fill the knowledge gap between external exposure and effect dynamics. The aim of the current work was to explain the impact of BPA on the immune response by determining its temporality. In addition, the relationship between BPA dose and these responses was investigated using a PBTK-TD model. Two experiments were performed on stickleback to characterize their biomarker responses, (i) a short exposure (14 days) at 0, 10 and 100 µg/L, including a depuration phase (7 days), and (ii) a long exposure (21 days) at 100 µg/L to measure the immunomarker dynamic over a long period. The fish spleens were sampled to analyze immune responses of stickleback at various times of exposure and depuration: leucocyte distribution, phagocytic capacity and efficiency, lysosomal presence and leucocyte respiratory burst index. At the same date, blood, muscle, and liver were sampled to quantify BPA and their metabolites (BPA monoglucuronide and BPA monosulfate). All these data enabled the development of the indirect pharmacodynamic models (PBTK-TD) by implementing the responses of biomarkers in the existing BPA PBTK of stickleback. The results shown a high induction of phagocytosis activity by BPA in the two exposure conditions. Furthermore, the immunomarkers exhibit very different temporal dynamics. This study demonstrates the need of a thorough characterization of biomarker response for a further use in Environmental Biomonitoring.

Keywords : PBTK-TD model, immunomarker, phagocytosis, fish, BPA, three-spined stickleback.

1. Introduction

Bisphenol A (BPA) is one of the most used and studied endocrine-disrupting compounds (EDCs) worldwide (Faheem and Bhandari, 2021). In 2015, the European Food Safety Authority (EFSA) evaluated the Tolerable Daily Intake (TDI) of BPA to be equal to 4000 ng/kg body weight and more recently, the European Commission classified this chemical as a substance of very high concern (SVHC) (Ougier et al., 2021).

In response to the concerns regarding adverse outcomes that could result from daily exposure to BPA and stricter legislation, industries have started to replace BPA with various structural analogs (Oliviero et al., 2022). Nevertheless, production volume of BPA remains high (Faheem and Bhandari, 2021; Samuel et al., 2022). Accidental direct or indirect release from wastewater treatment or the natural deterioration of products containing BPA leads to its ubiquity in aquatic ecosystems. Most aquatic organisms are usually exposed to less than 1 µg/L, but waters near industrialized sites could lead to exposures of hundreds of µg/L (Flint et al., 2012). Thus, the continuous exposure of aquatic communities to BPA has been of great concern as highlighted by several publications describing its effects on the aquatic organisms.

As an EDC, the mode of action of BPA is based on its affinity with hormone receptors (estrogen receptors α and β) but BPA also acts as an antagonist of androgen~~ic~~ receptors and a disruptor of thyroid signaling (Faheem and Bhandari, 2021). It leads to the disruption of reproduction and growth processes in fish, which are extensively described in the literature (Crain et al., 2007; Faheem and Bhandari, 2021).

At the end of 2021, EFSA published a new proposal of TDI at 0.04 ng/kg body weight/day (EFSA, 2022) one hundred-thousand times lower than the TDI proposed in 2015. This new value was based on *in vitro* and *in vivo* studies in rat that concluded in immunotoxicity of BPA. Thus, exposure to this compound induced parameters involved in inflammatory reactions at various sites, including lungs and epididymis (EFSA, 2022). This recent update of the TDI by EFSA illustrates the understanding that EDC's adverse effects can be perceptible on biological parameters which are not directly related to reproduction. However, despite the close relationship existing between hormones and the immune system in fish, endocrine disruption effects of estrogenic compounds on the immune system are still poorly understood (Harris and Bird, 2000; Milla et al., 2011). Exposure to BPA results in complex immuno-modulatory effects in fish (Michałowicz, 2014). As in mammals, BPA could trigger inflammation by inducing pro-inflammatory markers like cytokines, chemokines and interleukins in zebrafish (Yang et al., 2015). However, at higher dose levels, exposure to BPA could lead to cell apoptosis and death. In addition to this complex relationship regarding the dose, a lack of interest concerning the temporal dynamic of immune markers was noticed in the literature. In general, most in vitro studies focus on the establishment of dose-response, *e.g.* in Yang et al. (2015), seven different doses of BPA were tested whereas immune parameters were only measured after 6h of exposure. Thus,

further investigations need to be performed to better understand the dynamics of immunomarkers over time and for various doses.

Biologically based mechanistic models can be used to predict and understand biomarker responses (Forbes et al., 2006). Indeed, traditional dose-response relationships are generally dependent on exposure time and route whereas mechanism-based approaches can be used to extrapolate to other exposure scenarios. In this context, a PBTK-TD model was specifically designed to describe both kinetics and immunomarker responses resulting from exposure to BPA. A PBTK model describing the ADME (Absorption, Distribution, Metabolization and Excretion) processes of BPA in fish has been previously developed (Mit et al., 2022). Notably, this model accurately predicted BPA and BPA metabolites levels in three-spined stickleback organs. An additional toxicodynamic (TD) component, that simulates the effects triggered by a substance or a mixture, was shown to provide better understanding of the toxicity mechanisms by testing hypotheses and, thus, to be potentially relevant for environmental risk assessment (Ling et al., 2005; Mit et al., 2021; Tebby et al., 2019). Thus, modelling responses of immunomarkers in a PBTK-TD model could help understand the relationship between the internal dose and the effect, identify the substance (parent or metabolites) responsible for the response and help characterizing its dynamics. This modelling approach would inform both the temporality of the response, and dose-responses relationships at a given time.

The aim of this study was to propose a PBTK with TD sub-models describing immunomarker dynamic responses. TD data were obtained from two exposures to BPA performed on fish in laboratory. An analysis of the immunomarkers was completed prior to their selection and the application of the appropriate TD models. Indirect response models were compared to test hypotheses regarding dose-dependency and the non-trivial temporal dynamics of biomarker modulation.

2. Materials and methods

The PBTK model in which immune responses are integrated was reported previously in Mit et al., 2022 where full details of the experimental approach and model development can be found. Immune responses from spleen samples from the same fish previously exposed to BPA are evaluated here to build on previous work and to gain insight into how BPA and its metabolites affect immunity in fish. An additional experimental dataset is added in the current paper and further denominated as "long exposure".

2.1. Stickleback experimental data

Experimental protocols were conducted following the European directive 2010/63/UE for the protection of animals used for scientific purposes at INERIS, registration number E60-769-02. The experimental protocols were submitted and reviewed by a French nationally recognized ethical committee, CREMEAPS, registration number 96. Two experiments were performed, (i) a short exposure (14 days) at two different concentration levels including a depuration phase (7 days), and (ii) a long-exposure (21 days) at one concentration level to measure the immunomarker dynamics over a long period (Table 1). In the first experiment (i), internal concentrations and immune responses were measured in three spined stickleback, while in the second (ii), only the immune response was measured. Prior to each experiment, fish sex was determined using a mathematical model which distinguish male from female based on their head morphology (de Kermoysan et al., 2013). Mature fish sexually inactive (found in the field outside the breeding season) were selected to avoid confounding effects that could be introduced by sexual competition between males or females.

Table 1. Description of the two experiments on threespined stickleback

Exposure	Models (biological matrix)	BPA nominal concentration in water (µg/L)	Experimental Schedule (day)	Metabolites	Fish parameters
Short	TK (Liver, blood, carcasse) TD (spleen)	0, 10,100	7d uptake 7d depuration	BPA glu BPA sulf	n = 380 48.8 ± 4.4 mm 1.7 ± 0.4 g
Long	TD (spleen)	0, 100	21d uptake	na	n = 140 52.9 ± 5.9 mm 1.8 ± 0.6 g

2.1.1. Short-exposure experiment (14 day)

This experiment was previously described in details in Mit et al. (2022). This experiment consisted of seven days of exposure to BPA and seven days of depuration (fish in clear water). Shortly, adult (i.e. mature gonads) but sexually inactive sticklebacks with the same life history (similar age, n = 380,

48.8 ± 4.4 mm; 1.7 ± 0.4 g; sex ratio 1:1) were obtained from the INERIS husbandry (Verneuil-en-Halatte, France). At the beginning of the experiment, fish were randomly distributed into 8-L tanks with ten fish per tank and a 1:1 sex:ratio (16 ± 1°C, 350 µS/cm, photoperiod of 12:12 h) in a continuous flow system (≈ 1 L/h). Fish were fed daily with frozen blood worms, except the day before they were sampled. After five days of acclimation, fish were exposed for seven days to BPA (99% purity, 0, 10, and 100 µg/L, CAS number 80-05-7, Sigma). Water was randomly sampled several times (at 2, 4, 8, 24, 48, 72, and 168 hours) and analyzed with LC-MS/MS (previously described in Mit et al. (2022)). During exposure, all the fish from two tank for each condition, *i.e.*, 20 fish (ten females and ten males) were sampled at 5, 24, 48, 96 and 168 hours. After the end of the exposure, the remaining fish were sampled at 24 hours and 168 hours (192 and 336 hours since the beginning of the experiment, respectively). At each sampling time, fish were anaesthetized (tricaine methanesulfonate, 100 mg/L, Sigma), sacrificed, measured, weighed. The blood, the liver and the carcass were used to measure BPA and BPA metabolite concentrations; spleens were collected to measure immunomarkers.

2.1.2. Long-exposure experiment (21-day)

After five days of acclimation, adult (i.e. mature gonads) but sexually inactive sticklebacks with the same life history (similar age, n = 140, 52.7 ± 5.6 mm, 1.8 ± 0.6 g, sex ratio 1:1) were exposed for 21 days at 0 and 100 µg/L of BPA (nominal concentration). At the beginning of the experiment, males and females were separated to avoid stress and were randomly distributed into 8-L tanks with ten fish per tank and a 1:1 sex:ratio (16 ± 1°C, 350 µS/cm, photoperiod of 12:12 h) in a continuous flow system (≈ 1 L/h). Fish were fed daily with frozen blood worms, except the day before they were sampled. Water samples were taken from the tanks at 1, 3, 8, 15 and 21 days and BPA level was analytically measured. At 7, 14 and 21 days of exposure, all the fish of two tanks for each condition, *i.e.*, 20 fish (ten females and ten males) were sampled. Fish were anaesthetized (tricaine methanesulfonate, 100 mg/L, Sigma), sacrificed, measured, weighed and spleens were collected to measure immunomarkers.

2.1.3. Innate immune biomarker analysis

As previously described by Bado-Nilles et al. (2014), each spleen was pressed through sterilized nylon mesh (40 µm, Sigma-Aldrich, USA) with Leibovitz 15 medium (L15, Sigma-Aldrich, USA) completed with heparin lithium (100 mg/L, Sigma-Aldrich, USA), penicillin (500 mg/L, Sigma-Aldrich, USA) and streptomycin (500 mg/L, Sigma-Aldrich, USA). The leucocyte suspension was stored at 4°C for 18 h before analysis to prevent bias due to grinding stress. Measurements were performed on whole leucocytes using a MacsquantX flow cytometer (Miltenyi Biotec, Bergisch Gladbach, Germany). To allow comparison between each sample, the leukocyte concentration was normalized to 10^6 cells/ mL of culture medium.

A complete description of the protocols used to measure by flow cytometry the different immunomarkers can be found in Marchand et al. (2017) and Catteau et al. (2019). In the present work,

we measured the leucocyte distribution (lymphocyte and granulocyte-macrophage percentages), the cellular mortality (apoptotic and necrotic cell percentages), the phagocytosis activity (phagocytic capacity and efficiency, lysosomal presence (Mean Fluorescent Intensity, MFI) and leucocyte respiratory burst index (ratio of phorbol 12-myristate 13-acetate stimulated cells over unstimulated cells, the latter being also denominated as inactivated reactive oxygen species level). A complete description of the different immune protocols used is provided in supplementary information (SI).

2.2. Model structure

2.2.1. General structure

The model structure of the PBTK-TD (Figure 1) was derived from the PBTK described in Mit et al. (2022). Briefly, this PBTK was adapted to take into account BPA ADME processes. BPA absorption was assumed to occur exclusively through the gills and to be distributed via the plasma in 12 well-mixed compartments. Metabolization was considered as the main process of excretion and to occur in both liver and venous plasma. Remaining BPA was assumed to be excreted through the gills. The two predominant metabolic conjugates, BPA glucuronide (BPA gluc) and BPA sulfate (BPA sulf), were then distributed in five well-mixed compartments. BPA metabolite excretion was assumed to occur only through the bile.

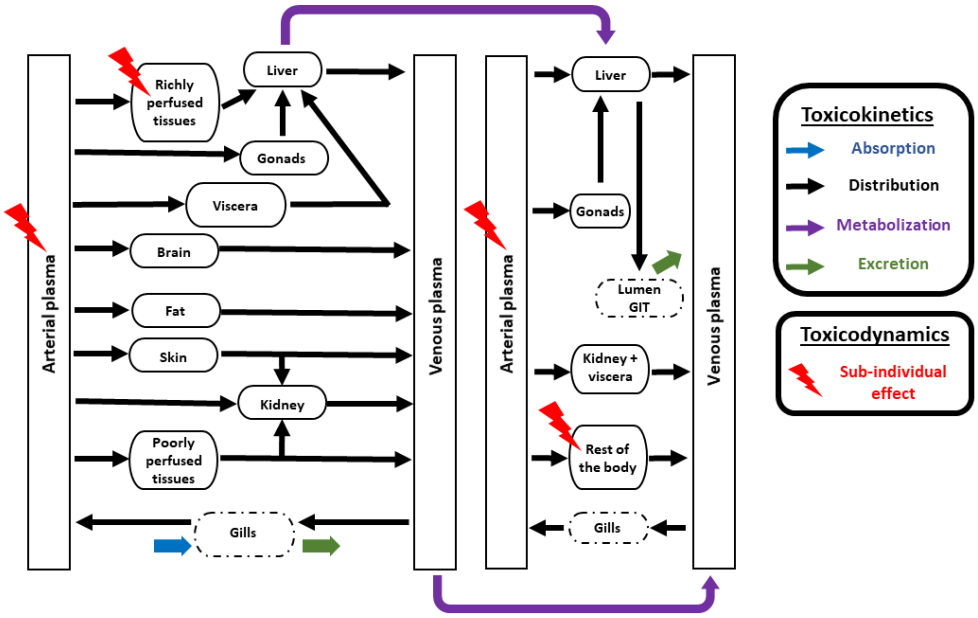

Figure 1. Schematic representation of the physiologically based kinetic model coupled to the toxicodynamics of bisphenol A. Uptake by the gills is symbolized in blue. Metabolization occurs in the liver and in venous plasma (purple). Excretion by the gills and the feces *via* the bile is symbolized

in green. The toxicodynamics of BPA are implemented in the compartments where effects are measured.

2.2.2.TD sub-models

As innate immune parameters were measured in spleen, the different TD sub-models were implemented in the richly perfused (RP) compartment. Indeed, it was considered to be the compartment with the plasma flow the closest to the spleen. Alternatively, arterial plasma concentration was tested as a proxy for the spleen concentration.

A specific class of basic indirect response models was chosen to simulate immunomarkers over time (formally described by Dayneka et al. (1993)). Indeed, contrary to direct responses which are directly affected by a chemical, indirect responses show a lag time after the interaction of the chemical at the site of action. This type of mechanistic model was recommended to describe a response modulation (loss or stimulation) depending on a chemical-receptor interaction (Felmlee et al., 2012).

$$\frac{\mathrm{dR}}{\mathrm{dt}} = \mathrm{K_{in}} - \mathrm{K_{out}} \times \mathrm{R} \qquad \text{(Equation 1)}$$

Equation 1 describes the measured response R in normal conditions. K_{in}corresponds to a zero-order production rate of the response variable and K_{out} to a first-order rate of the loss of the response. In exposed conditions, a stimulation (Equation 2) or an inhibition (Equation 3) can modulate one of the two rates (Dayneka et al., 1993) (*i.e.*, multiplication of the rate by S(t) or I(t)).

$$\mathrm{S(t)} = 1 + \frac{\mathrm{S_{max}} \times \mathrm{C_{i,t}}}{\mathrm{SC_{50}} + \mathrm{C_{i,t}}} \qquad \text{(Equation 2)}$$

$$\mathrm{I(t)} = 1 - \frac{\mathrm{C_{i,t}}}{\mathrm{C_{i,t}} + \mathrm{IC_{50}}} \qquad \text{(Equation 3)}$$

With S(t) a stimulation function and I(t) an inhibitory function. $C_i(t)$ represents the concentration in the tissue *i* (alternatively in RP, C_{rp} or in plasma C_p) at the time t. S_{max} the maximum effect attributed to the chemical, SC_{50} the chemical concentration producing 50% of the maximum stimulation and IC_{50} the chemical concentration producing 50% of maximum inhibition.

Regarding a potential phenomenon of hysteresis between internal concentration variations and measured response modulations, an additional modification was proposed based on the work of Sheiner et al. (1979). Thus, a better description of the response could be achieved by replacing C_i in Eq.2 or Eq.3 with the concentration corresponding to a virtual compartment *D* to account for the observed delay (see Equation 4).

$$\frac{\mathrm{dD_i}}{\mathrm{dt}} = \mathrm{k_{delay}} \times (\mathrm{C_i} - \mathrm{D_i}) \qquad \text{(Equation 4)}$$

With k_{delay} a dimensionless constant. Finally, to take into account a potential loop regulation of the measured response during the exposure, a feedback sub-model was implemented based on the work of

Bundgaard et al. (2007). Depending on the measured response, a modulation variable was added to suppress the stimulation or inhibition of the response at a given time.

$$M = (t - \tau) \times k_{tol} \quad \text{(Equation 5)}$$

With M the modulator, t the time, τ the time at which the feedback starts and k_{tol} a modulatory constant.

The equation 6 is given as an example of a model integrating a modulator and a virtual compartment for a production stimulated response with D_{rp} being the damage produced by the concentration of chemical in the richly perfused tissue.

$$\frac{dR}{dt} = K_{in} \cdot \left(1 + \frac{S_{max} \times D_{rp}}{SC_{50} + D_{rp}}\right) \times \frac{1}{M} - K_{out} \times R \quad \text{(Equation 6)}$$

2.3. Biomarker response analysis and modeling

Calculations were performed using R version 3.6.1. (R Core Team, 2019) and GNU MCSim v6.2.0 (Bois, 2009). MCSim model codes were provided in SI (section 7).

2.3.1. Statistical analysis

Prior to modelling, a statistical analysis was performed for each immunomarker response. All responses were log-transformed. At each date, a one-way ANOVA followed by a post-hoc Dunnett test was used to detect significant differences between treated conditions and control. The level of significance for all the analysis was 5%. The biomarkers presenting the most consistent differences to control over time (*i.e.*, the dose-response was repeatedly observed during the exposure period) were then selected for the PBTK-TD modelling. Detailed statistical analysis for each endpoint is presented in SI (section 5).

2.3.2. Calibration of the biomarker responses

Based on the results of the statistical analysis, a combination of the TD sub-models was used to describe each selected biomarker response. For the calibration, all TK parameters were fixed and only TD parameters were calibrated (seven parameters for inactivated ROS and eight parameters for lysosomal presence and phagocytic efficiency). Most prior distributions were set as normal, and the coefficient of variation on the prior values was set to 30 % (including uncertainty and inter-individual variability). Mean prior values were retrieved from Marchand et al. (2019).

TD data corresponding to both short and long-exposure period were used to inform parameter posterior values. Prior to the calibration of the parameters using BPA TD data, control data were used to calibrate the baseline level of each response. TD models were calibrated on the geometric means of male and female altogether with the same weight for males and females. As described in Mit et al. (2022), BPA concentration levels in water that were used as input for the PBPK model were based on the measured concentrations. Other model inputs like initial fish weight and water temperature were set to the values

obtained by monitoring both experiments. Calibration was performed using Bayesian methods (Monte Carlo Markov Chains, MCMC). See all details in SI (section 6).

2.3.3. Comparison of the models

To determine which chemical, parent or metabolites, could be responsible for the measured responses, six versions of the model describing each biomarker were calibrated. In each model, one of the three simulated concentrations in RP compartment and arterial plasma (BPA, BPA gluc or BPA sulf) was used as input in the TD sub-model. In addition, the various models were calibrated on the observed ratio of the biomarker response in treated conditions over the control. Afterwards, Bayesian Inference Criteria (BIC), measuring goodness of fit and allowing the comparison of the different models, were calculated.

3. Results

In control aquarium, BPA and metabolites were below the detection limit (Table SI3). Measured BPA concentrations in water in the short experience were 5.0 ± 1.2 µg/L and 53.0 ± 19.3 µg/L (mean ± SD, nominal concentrations of 10 and 100 µg/L). During the long-exposure experiment, fish were exposed to 55.9 ± 6.3 µg/L (nominal concentration level 100 µg/L).

3.1. Innate immune parameter analysis

A total of nine immunomarkers was measured during the two experiments. No significant difference was observed between male and female for any measured parameters (see section 5 in SI).

3.1.1. Leucocyte distribution

Even if the percentages of granulocytes-macrophages tend to decrease throughout the experiment, only the highest dose at 0.25 day of exposure and the two doses on day 14 were significant. No significant response was found for the 21-day exposure (Figure 2).

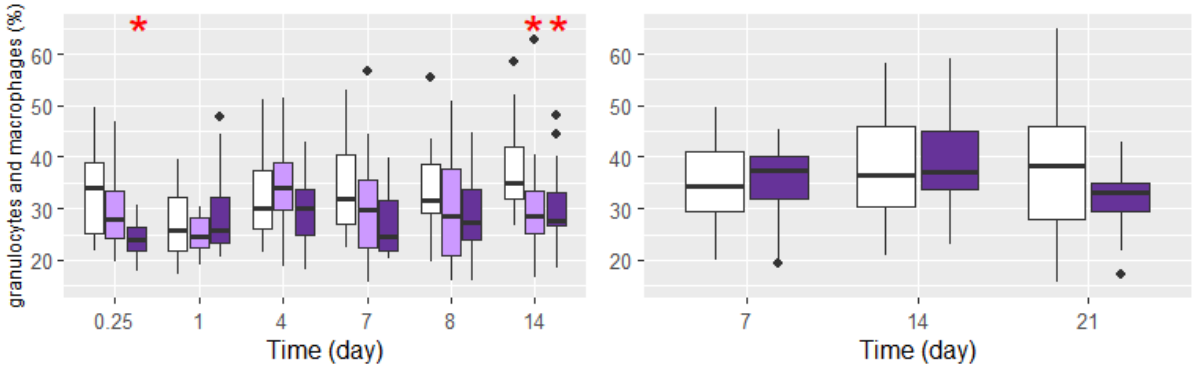

Figure 2. Leucocyte distribution (percentage of granulocytes and macrophages on leucocyte population) of three-spined stickleback during the short-exposure (left panel) and the long-exposure (right panel) experiments. *Asterisks* mark to statistically significant differences between control (blank) and treated conditions (10 µg/L of BPA in light purple and 100 µg/L of BPA in purple, n = 20).

3.1.2. Cellular mortality

Regarding cellular mortality, two parameters were measured, apoptotic and necrotic cell percentages (Figure 3). At the highest dose level (100 µg/L) a significantly higher percentage of cellular mortality (sum of apoptosis and necrosis percentages) was observed on day 1 in the short-exposure experiment (see SI section 5.2). No significant effect was observed during the depuration phase. In addition, no significant effect was observed during the 21-day experiment (Figure 3 right panel).

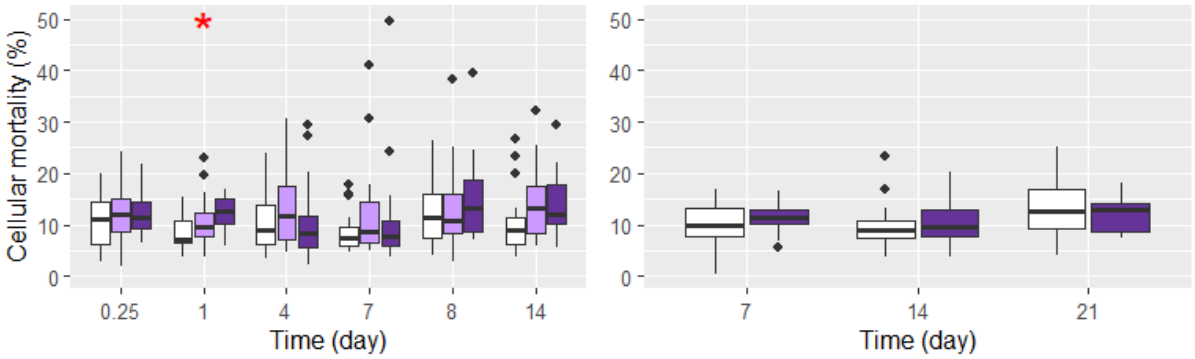

Figure 3. Cellular mortality (apoptosis and necrosis) of three-spined stickleback during the short-exposure (left panel) and the long-exposure (right panel) experiments. *Asterisks* mark to statistically significant differences between control (blank) and treated conditions (10 µg/L of BPA in light purple and 100 µg/L of BPA in purple, n = 20).

3.1.3. Phagocytic activity

Phagocytic activity concerned the attachment of the cell to foreign particles (phagocytic capacity), the internalization of the particle (phagocytic efficiency) (Figure 4), the lysosomal presence (Figure 5) and the respiratory burst (Figure 6). Overall, each parameter of phagocytic activity in exposed fish tends to increase compared to control fish. In fact, a significant induction in phagocytic capacity was measured on day 1 and day 8 for 100 µg/L for the short exposure (Figure 4A). This effect of induction was also found to be significant on day 7 for the 21-day exposure (Figure 4B). In terms of phagocytic efficiency, a significant induction was observed on day 1, 7 and 8 for the highest dose for the short exposure (Figure 4C) and also on day 7 for the 21-day exposure (Figure 4D).

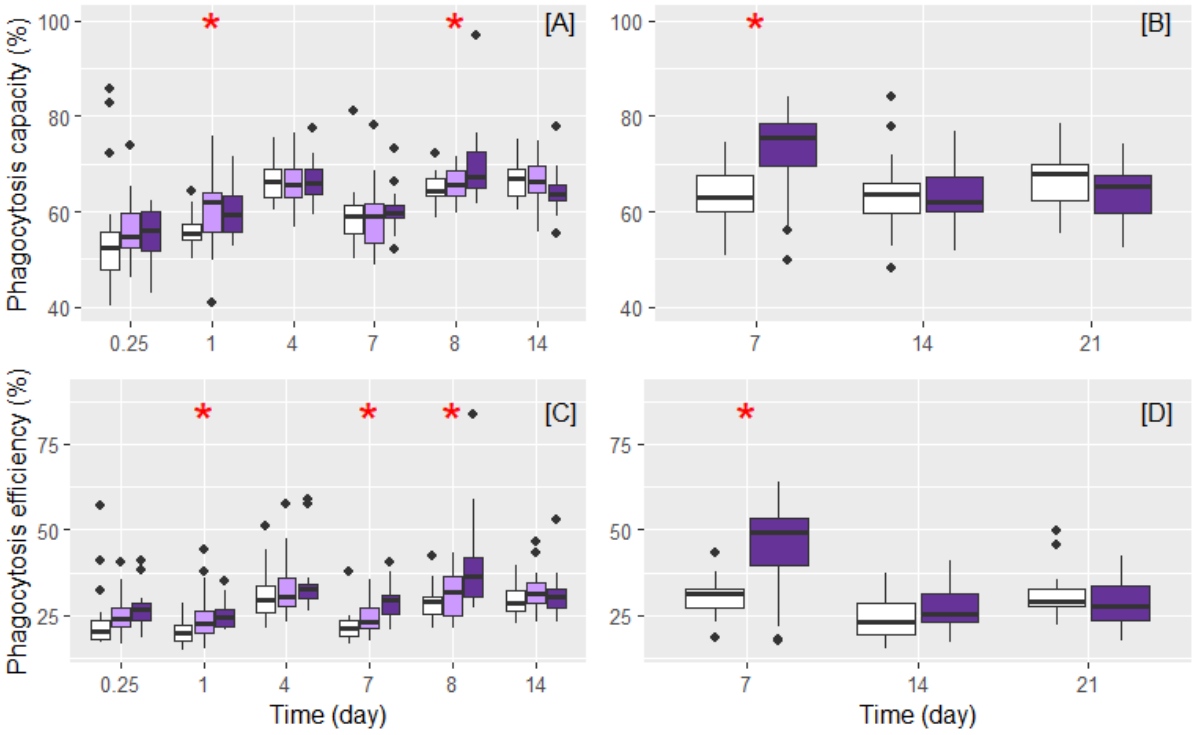

Figure 4. Splenic immune phagocytosis capacity (upper line) and efficiency (lower line) of three-spined stickleback during the short-exposure (right panel, A and C) and the long-exposure (left panel, B and D) experiments. *Asterisks* mark to statistically significant differences between control (blank) and treated conditions (10 µg/L of BPA in light purple and 100 µg/L of BPA in purple, n = 20).

During the short-exposure, an induction of lysosomal presence was significant on day 0.25 for both doses and the induction was also significant on day 1, 4 and 7 for the highest dose (Figure 5). During the depuration phase, this biomarker was significantly induced at both doses on day 8 and still induced on day 14 at the highest dose level (Figure 5). In the 21-day experiment, no significant effect was observed (Figure 5 right panel).

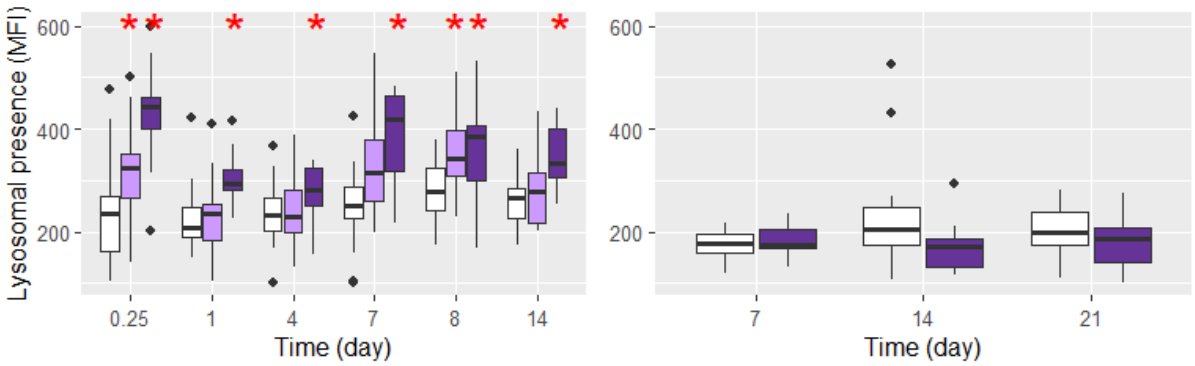

Figure 5. Splenic lysosomal presence during the short-exposure (left panel) and the long-exposure (right panel) experiments. *Asterisks* mark statistically significant differences between control (blank) and treated conditions (10 µg/L of BPA in light purple and 100 µg/L of BPA in purple, n = 20).

A significant induction of inactivated ROS levels at the two doses was observed on day 1 and only the highest dose on day 4 (Figure 6A). On day 7, all doses were significantly induced. During the depuration phase, the induction was significant for the highest dose level on day 8 (Figure 6A). Finally, inactivated ROS levels were induced at all doses on day 14 (Figure 6A). In the 21-day experiment, ROS B was significantly induced at all timepoints (Figure 6B).

Respiratory burst index (Figure 6C and D) was significantly induced at the highest dose level on day 0.25 and at the dose level 10 µg/L on days 1 and 4. On day 7, respiratory burst was significantly inhibited at dose level 10 µg/L (Figure 6C). During the depuration phase a significant induction of the respiratory burst was observed at both dose levels on day 8. For the long exposure, a significant inhibition was measured on days 7 and 14 (Figure 6D).

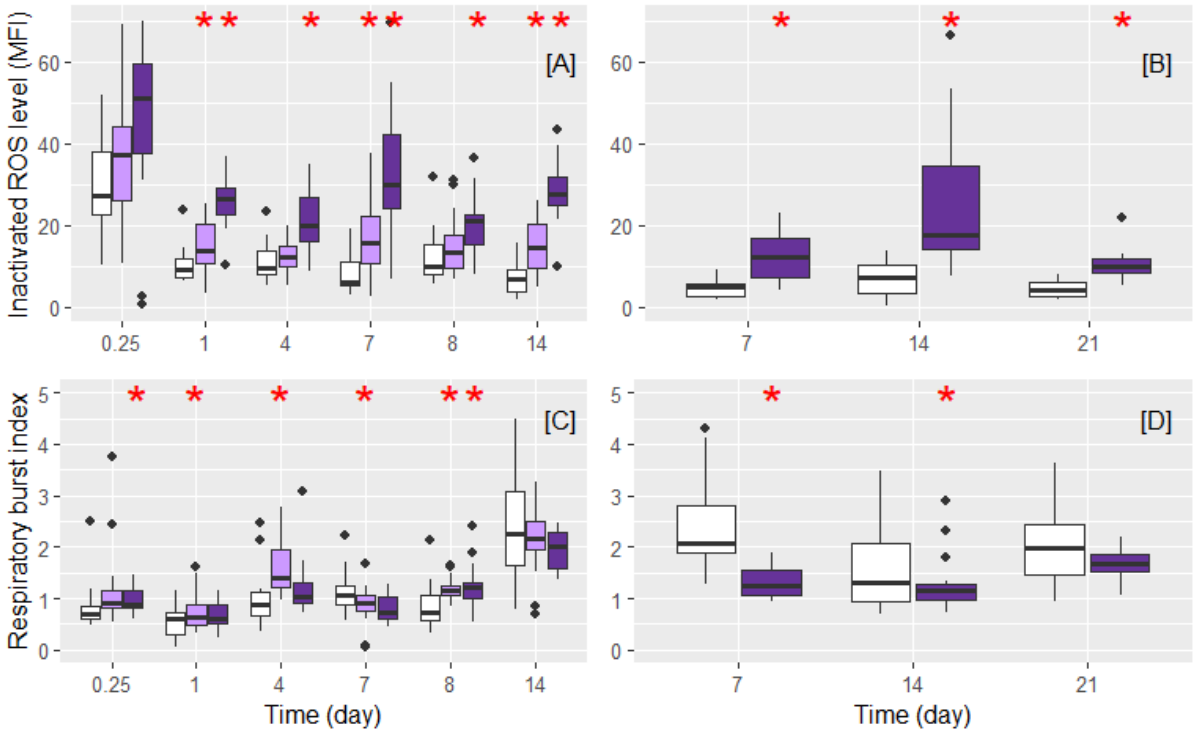

Figure 6. Respiratory burst of three-spined stickleback during the short (right-hand column, A and C) and the long (left-hand column, B and D) exposures. *Asterisks* mark statistically significant differences between control (blank) and treated conditions (10 µg/L of BPA in light purple and 100 µg/L of BPA in purple, n = 20).

3.2. Biomarker response modelling

Model inputs and parameters can be found in SI (table S11). Figure 7 presents the concentrations of BPA and BPA gluc predicted by the PBTK (Mit et al., 2022) for the two exposures both in plasma and richly perfused tissues. In the short experiment, a slower depuration kinetics of BPA glu in plasma (from day 7) was observed compared to the kinetic of the parent compound. Those predicted tissue concentrations represent the inputs of the different TD sub-models.

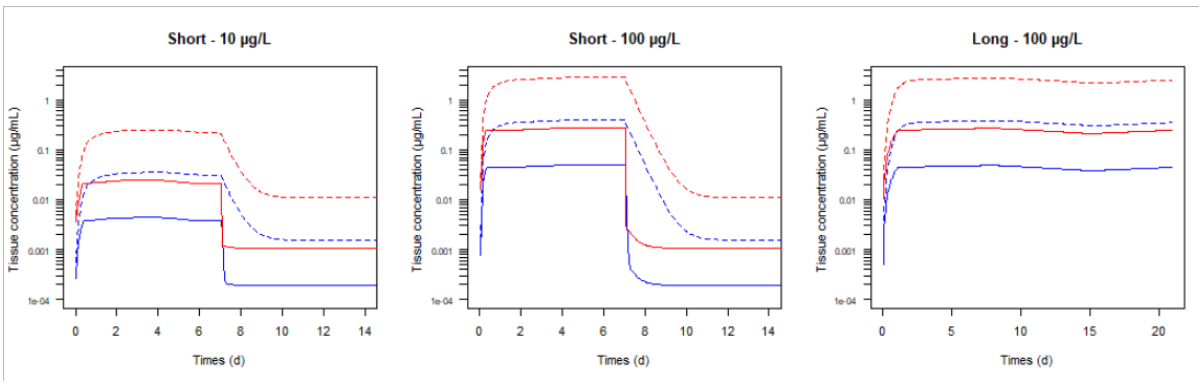

Figure 7. Richly perfused tissue (blue lines) and plasma (red lines) BPA and BPA glu concentrations for the short and long exposure. Full lines represent the BPA and dotted lines BPA glu.

Among biomarkers, two responses were selected: the phagocytic efficiency and the inactivated ROS level. Those biomarkers were chosen based on the consistency (*i.e.*, the dose-response was repeatedly observed during the exposure period) of their response over time.

Table 2 presents the comparison of the BICs calculated for each response using BPA or BPA metabolite in RP tissues and arterial plasma as model inputs. The lowest BIC was observed when phagocytic efficiency was modelled with BPA gluc concentration in arterial plasma used as an input. Regarding inactivated ROS modeled responses, the lowest BIC was obtained with BPA concentration in arterial plasma as input.

Table 2. Comparison of the Bayesian Information Criteria (BIC) obtained for the two different modeled immune parameters. Each response was calibrated using the concentrations of BPA and its metabolites in RP tissues or in plasma as input in the toxicodynamic model.

	BPA		**BPA gluc**		**BPA sulf.**	
	RP Tissues	**Plasma**	**RP Tissues**	**Plasma**	**RP Tissues**	**Plasma**
Phagocytic efficiency	-25.2	-28.1	-28.5	**-34.1**	-23.0	-23.1
Inactivated ROS	47.7	**43.4**	44.4	45.4	55.4	53.1

The phagocytic efficiency and inactivated ROS were induced by BPA or its metabolites. Therefore, the Equation 2 mimicking a response stimulation was chosen to model each biomarker response (Figure 8, 9 and 10).

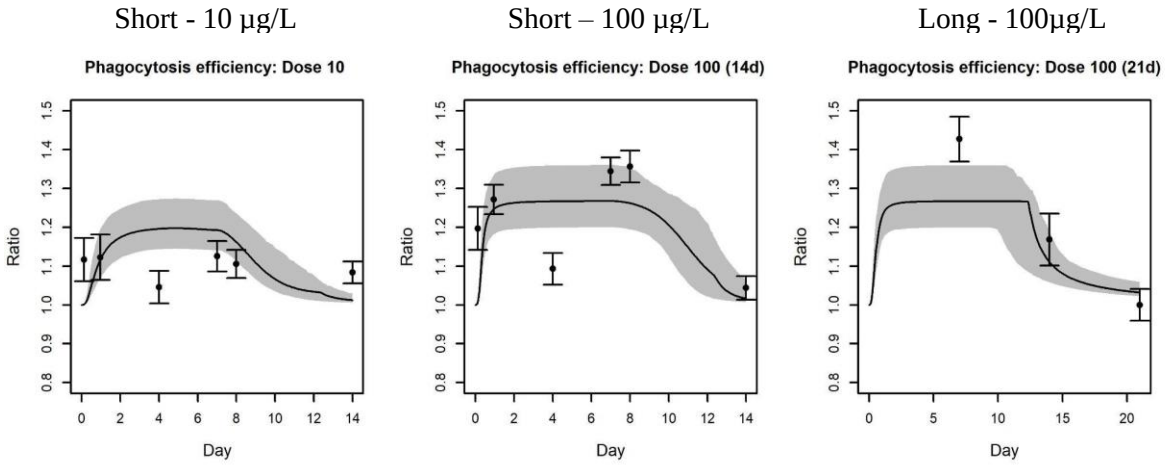

Figure 8. Phagocytic internalization efficiency ratio simulated by the PBTK-TD model (Equation 6) based on the BPA gluc concentration in arterial plasma for the short and long exposure. The solid lines represent the model simulations and the dots the ratio (treated conditions over controls) of the

response. The grey area is the 95% credibility interval computed from the posterior distributions. The simulations were made using the last 333 iterations of the three MCMC chains. Error bars represent the standard deviation on the observed ratios.

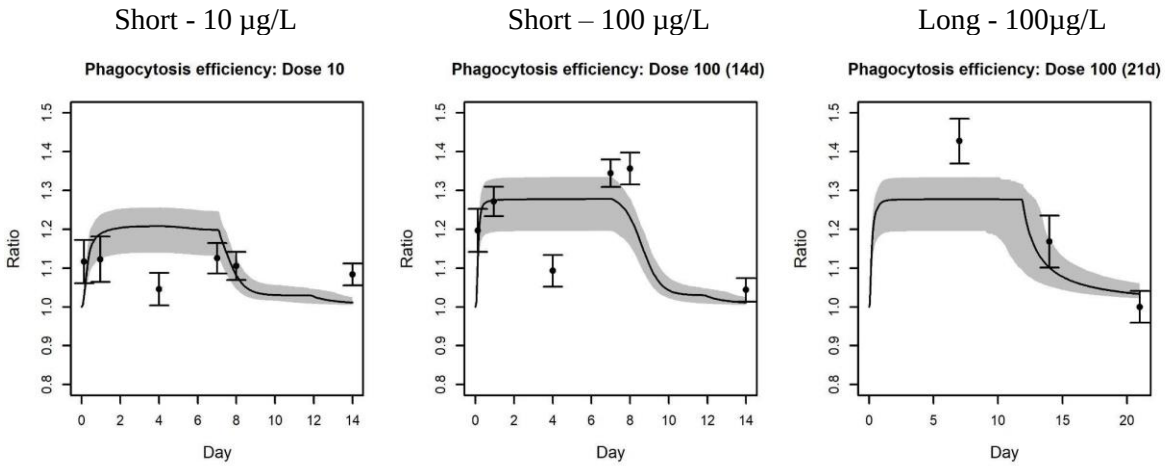

Figure 9..Phagocytic internalization efficiency ratio simulated by the PBTK-TD model (Equation 7) based on the BPA gluc concentration in arterial plasma for the short and long exposure. The solid lines represent the model simulations and the dots the ratio (treated conditions over controls) of the response. The grey area is the 95% credibility interval computed from the posterior distributions. The simulations were made using the last 333 iterations of the three MCMC chains. Error bars represent the standard deviation on the observed ratios

Phagocytic internalization efficiency was best modelled using BPA gluc concentration in arterial plasma and a loop regulation.

More precisely, model backward selection (Table S12 in SI) showed that the models integrating a virtual compartment to add a delay (Equation 6, Figure 8) or based directly on the BPA gluc concentration in arterial plasma (Equation 7, Figure 9) provide similar results, with a slightly lower BIC for the latter. However, focusing on the end of the exposure, without delay, the response stability observed between the day 7 and 8 is less accurately modelled.

$$\frac{dR}{dt} = K_{in} \cdot \left(1 + \frac{S_{max} \times C_{art\ glu}}{SC_{50} + C_{art\ glu}}\right) \times \frac{1}{M} - K_{out} \times R \qquad \text{(Equation 7)}$$

Once calibrated, both TD model provide accurate predictions with a mean fold equal to 1.079 and 1.076, respectively. The predicted phagocytic internalization efficiency at nominal dose level 10 µg/L showed a mean induction of 15% compared to control (Figure 8 and 9). 73% of the observed points were within the 95% prediction interval. However, phagocytic internalization efficiency was under-predicted at 14 days, highlighting a high observed level of induction even after seven days of depuration. Both in the short-exposure and the long-exposure experiments at nominal dose level 100 µg/L, the predicted

induction in treated conditions was around 25% greater than the control. The data were correctly fitted, including the 14-day point during the depuration. However, comparing the point measured on day 7 at nominal dose level 100 µg/L in the short and long-exposure experiment (Figure 7) with the plateau simulated by the model, it reveals an underprediction of the model, and a quite good reproducibility of the induction between the two experiments. Model calibration seems to have led to a tradeoff between the accuracy in low and high dose at this time point. Finally, the loop regulation integrated in our model (Eq.5) correctly fitted the return to the baseline between day 7 and day 21.

Regarding inactivated ROS, Equation 4 was simplified so that no depuration occurred in the virtual compartment (Equation 8) and no loop regulation was introduced (see Equation 9).

$$\frac{\mathrm{d}D_{rp}}{\mathrm{d}t} = k_{delay} \times C_{rp} \qquad \text{(Equation 8)}$$

$$\frac{\mathrm{d}R}{\mathrm{d}t} = K_{in}.\left(1 + \frac{S_{max} \times D_{rp}}{SC_{50} + D_{rp}}\right) - K_{out} \times R \qquad \text{(Equation 9)}$$

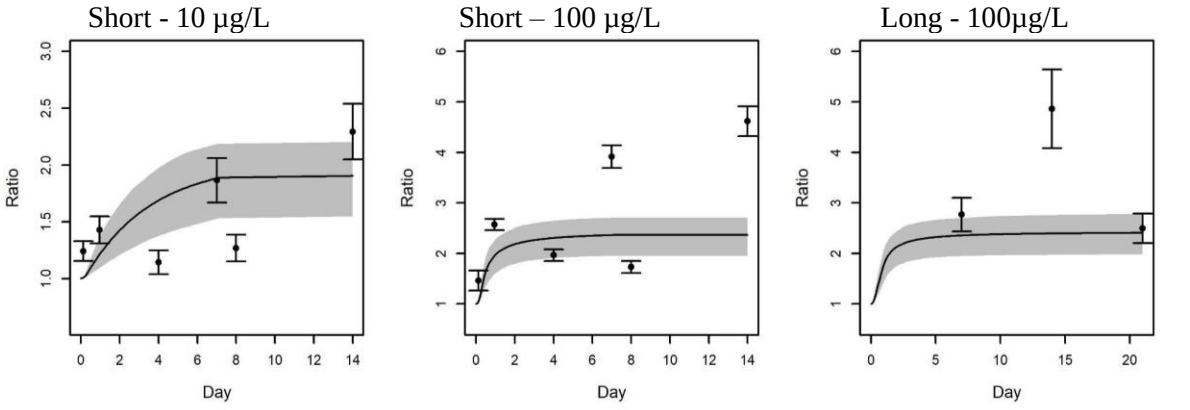

Figure 10. Inactivated ROS level ratio simulated by the PBTK-TD model based on BPA plasma concentration for the short and long exposure. The solid lines represent the model simulations and the dots the ratio (conditions over controls) of the response. The grey area is the 95% prediction interval, computed from the posterior distributions. The simulations were made using the last 333 iterations of the three MCMC chains. Error bars correspond to the standard deviation on the mean ratios.

Once calibrated, TD model provide accurate predictions with a mean fold equal to 1.38. The inactivated ROS response (Figure 10) was quite different and showed a continuous increase during the exposure period in both experiments. Steady states were reached only after the short exposure, once the exposure stopped (mean ratio around 25% higher than the control for the 10 µg/L dose level and around 120% at the 100 µg/L dose level). Consequently, in the 21-day experiment, the mean ratio predicted by the model reached 300% of the control at 21 days of exposure. Our simulations stressed an important variability regarding the responses over time. The simple equations included in our model failed to predict the large increases and decreases between successive timepoints observed during each exposure.

4. Discussion

The present work is part of a continuous effort made in ecotoxicology to improve the characterization of biomarkers. In Forbes et al. (2006), the use and limitations of those tools was discussed. Among the main concerns on the subject, the difficulty to untangle their biological variability due to confounding factors (sex, season, species…) and the actual effect of xenobiotics was highlighted. One of the solutions proposed in this work was to build mechanism-based models integrating relevant sub-individual parameters. In our paper, toxicodynamic sub-models were implemented in a PBTK specific to BPA. In parallel, two exposures to BPA were performed. One exposure (the short exposure) was described previously in Mit et al., 2022 and the other (the long exposure) was described in this work. The monitoring of immunomarkers in both experiments is presented for the first time in this paper. A selection of the responses measured in fish were then modeled using the PBTK-TD.

So far, inconsistent results regarding BPA effects on innate immune parameters were described in the literature (Pandey et al., 2018; Yang et al., 2015). Nevertheless, in line with other research, the present study demonstrated the immunomodulatory potential of BPA. Here, we showed that phagocytic activity of splenic leukocytes taken from fish exposed to BPA was induced following a dose dependent relationship and this effect was measurable quickly after the beginning of the exposure. In Yang et al. (2015), this induction was also observed in trout head kidney macrophages exposed *in vitro* during 6 h to 1 and 10 µg/L of BPA. Interestingly, in Yang et al. (2015) at higher doses, phagocytic activity was significantly inhibited showing a non-monotonic dose response (NMDR). On the contrary, in *Channa punctatus,* another teleost fish, the phagocytic activity was significantly inhibited *in vitro* after 16 h of exposure even at low dose (from 0.229 µg/L to 229 µg/L) (Pandey et al., 2018).

In the current study, both phagocytosis capacity and efficiency, lysosomal presence and respiratory burst were also measured. The lysosomal presence was significantly induced but the respiratory burst dynamic was not monotonic over time. Depending on the studies, the respiratory burst was reported to be induced (Faheem and Bhandari, 2021; Samuel et al., 2022; Yang et al., 2015) or inhibited (Bado-Nilles et al., 2014; Yin et al., 2007). In fact, BPA was shown to modulate various genes associated to the NF-κB signalling pathway. BPA up-regulates pro-inflammatory cytokine genes such as Tumor Necrosis Factor α *(tnf-α),* involved in the enhancing response of phagocyte respiratory burst (Faheem et al., 2020; Faheem and Bhandari, 2021). On the contrary, at higher dose, BPA immunosuppression was demonstrated in various species, including *Gobiocypris rarus* and *Labeo rohita* larvae (Faheem et al., 2020; Tao et al., 2016). Some hypotheses could be proposed to explain those contradictory results. As it was highlighted previously, it is generally assumed that the immunomarker dynamic is stable over time, but it was shown here that it depends on the biomarker considered. Another hypothesis could be a differential expression of estrogen receptor *α* and β depending on tissue type resulting in discrepancies in response measured in splenic or head kidney macrophages (Bado-Nilles et al., 2014; Filby and Tyler, 2005). Indeed, leucocytes and, in particular, macrophages possess estrogen receptors (ERs) (Casanova-

Nakayama et al., 2011; Massart et al., 2014) and NF-κB and ERs were linked to the immunomodulating effect of BPA (Yang et al., 2015).

The PBTK specific to BPA and calibrated on TK data measured in three-spined stickleback used in this study was presented in a previous work (Mit et al., 2022). While PBTK are often used as a basis when studying effects in toxicology, the approach presented here is still scarce in ecotoxicology (Abbas and Hayton, 1997; Liao et al., 2005; Ling et al., 2005; Liu et al., 2014; Mit et al., 2021; Tebby et al., 2019; Zhang et al., 2019). Yet, PBTK models offer many advantages compared to simpler TK model, in particular, when considering effects at the sub-individual level, the predictions of internal concentrations in target organs could improve greatly the accuracy of the modeled response (Grech et al., 2017; Mit et al., 2021; Zhang et al., 2019). In addition, contrary to most dose-response studies which used static model, our study describes the response over time. In terms of effect, most of studies in the field of ecotoxicology are focusing on three endpoints, namely survival, reproduction, and growth. However, the impacts at the individual level can be considered as late effects when applying to biomonitoring or to the evaluation of substances inducing non-directly lethal effects, like EDCs. In this context, the development of models integrating early responses, like PBTK-TD, are needed. Moreover, our work coupling experimental and modelling approaches enabled to highlight the discrepancy of some datapoints that could be mistaken for an actual particular response whereas it is probably an artifact due to experimental issues. For example, the measured phagocytic efficiency on day 4 for both doses for the short-exposure experiment sounds incoherent with the mechanisms assumed by model and supported by the other datapoints.

Only few models have integrated biomarker responses in ecotoxicology, the first one being the PBTK-TD developed by Abbas and Hayton (1997) and describing the inhibition of AChE by chlorpyrifos in rainbow trout. In this model, the response was a consequence of the dynamic of enzyme synthesis, degradation, and inhibition. In our case, the mechanisms underlying the immunomarker responses were unknown. For this reason, a class of indirect toxicodynamic models was chosen (Dayneka et al., 1993). Nevertheless, the dynamics that were observed when measuring immunomarkers over time showed the limitations of those indirect models. As it is often observed in the literature, there was a discrepancy between the internal concentration and the response (Lee et al., 2002). However, even if the measured responses were sometimes slow to dissipate, most responses were quickly triggered. It was for example the case for the phagocytosis activity. In this respect, indirect models were unable to correctly simulate this dynamic. In addition, the implementation of the virtual compartment based on the work of Sheiner et al. (1979) was insufficient to perfectly fit the measured data since the modeled responses were triggered too slowly. The simulations showed that the best model was probably a trade-off between a basic indirect model and its updated version including the virtual compartment. Another process highlighted by our PBPK-TD modeling approach was the feedback phenomenon measured in the long exposure for some markers. For this reason and according to Bundgaard et al. (2007), the return to the

basal value under exposure was introduced in the TD model. The mechanism underlying this dynamic is unclear. However, it is possible that in the absence of actual infection, the organism is able to modulate the response triggered by BPA to prevent energy waste. Nevertheless, for other responses like the production of ROS involved in the destruction of pathogens, the mechanism dynamic seems to be controlled by another mechanism.

One key issue during the development of a PBTK-TD is the amount of data needed to inform both the TK and the TD of the substance of interest. In Mit et al. (2022), the levels of BPA and BPA metabolites were measured in three organs, at several times and for two doses. The design of this study, including uptake and depuration, was chosen to inform ADME parameters. Considering the toxicodynamic part presented here, two experiments were performed. The first one with a 7-day exposure followed by a 7-day depuration (same experiment for TK) was selected to evaluate the earliness of the response and its potential return to basal value after exposure. The second one, the long-exposure experiment, was selected to determine how the biomarkers of interest would evolve over a longer period. As it can be noticed with our selection of immunomarkers, the dynamic of the responses were heterogenous. Notably, biomarkers describing phagocytosis showed the importance of conducting the most complete study when measuring biomarker dynamic. Thus, non-monotonic responses over time can be identified as it was the case for phagocytosis efficiency or lysosomal presence. Regarding dose-response, only a selection of several doses, over a sufficiently large range of concentrations, would allow the identification of potential non-monotonic dose responses (Beausoleil et al., 2013; Vandenberg et al., 2012). In our case, fish were exposed to two doses of BPA (plus the control). Given the limited number of concentrations, it was not possible to conclude about the shape of the dose-dependency of the different responses, even if some inducted or inhibited responses were highlighted over the small range of tested concentrations. In fact, in Beausoleil et al. (2013), BPA, as most of EDCs, was characterized by NMDR for a variety of effects. Considering our results, it is interesting to note that the existence of a feedback phenomenon or a potential desensitization of a receptor could be mistakenly interpreted as for a dose dependency whereas the measured response appears to be unstable over time (Beausoleil et al., 2013).

For each immunomarker, one of the three simulated concentrations in RP compartment and arterial plasma (BPA, BPA gluc or BPA sulf) was used as input in the TD sub-model. The lowest BIC was observed regarding inactivated ROS with BPA concentration in arterial plasma as input, whereas the BPA gluc concentration in arterial plasma provides the lowest BIC regarding phagocytic efficiency. In human, one recent experimental work has examined the in vitro effects of BPA and BPA gluc on glycolysis and functional responses of neutrophils (Peillex et al., 2021). Contrary to our results, the authors found no effect of BPA nor BPA gluc on phagocytosis and ROS production. Nevertheless, BPA gluc was identified as a potentially higher disruptor than its parent. Furthermore, in this work, the short timeframe of the experiment and an extensive literature regarding the immunotoxic effects of BPA was stressed to balance the conclusion about the absence of effect of BPA gluc. In lines with the disrupting

potential of BPA gluc, Boucher et al. (2015) showed the potential of the metabolite to induce adipogenesis in both murine and human cells.

Mixture of the parent compound and the metabolites could be also assumed to be responsible for the toxic effect. This assumption could be tested using the PBTK-TD model to predict dose-response curves for equitoxic mixtures where each chemical contributes equally to the total toxicity (Mit et al. 2021). However, an equitoxic mixture seems a bit speculative, and more data have to be obtained on the toxicity of the isolated metabolites to explore some possible interactions. Nevertheless, it is important to note that if the effect is better explained by the concentration of one of the substances, this does not exclude a lesser effect of the other and thus a combined effect of the mixture.

Currently, biomarkers are used in environmental biomonitoring to assess the health of aquatic ecosystems (Catteau et al., 2021; Catteau et al., 2022). Following the different points highlighted by Forbes et al. (2006), a continuous work was performed to reduce the uncertainty induced by the confounding factors complicating the use of biomarkers. In our work, the focus was made on the temporal dynamic of the biomarkers. The variety of biomarker temporal dynamic obtained under the same exposure conditions stressed the need to study the impact of time on biomarkers measure as frequently as it is for the dose-response. Indeed, the characterization of the time-dependency and knowledge of the variability of the response between biomarkers provide opportunity to propose various hypothesis regarding the mechanisms underlying the different responses. For example, comparing stable and unstable biomarker responses over time (*e.g.* inactivated ROS and phagocytic efficiency) can provide information on the dynamics of the underlying stress.

In addition to a better understanding of the dynamics of innate immune parameters currently used in biomonitoring (Bado-Nilles et al., 2014; Catteau et al., 2021), the integration of those responses in a PBTK-TD will benefit the current effort of bringing together existing data to support ecotoxicological risk assessment in building quantitative adverse outcome pathways (Ankley et al., 2010; David et al., 2019). In this work, the modulation of immune parameters was not linked to any notable detrimental effects affecting three-spined stickleback. However, the triggering of innate immune defence, as observed here, is energetically costly (Pandey et al., 2018) and could result in a trade-off with other biological functions. However, in Spromberg and Meador (2006), the modeling of immune suppression resulting from an exposure to low dose of toxicants was supposed to only impact the ability to resist to pathogens and therefore to impact survival. Conversely, in stickleback, it was shown that the infection resistant offsprings resulting from the mating of brightly colored male were growing slowly supporting the idea of trade-offs between growth and immunity (Barber et al., 2001). Finally, the proven bidirectional communication between immunity and neuroendocrine systems taken with the known disturbance of immune responses during reproduction support the idea of trade-off between reproduction and immunity (Bado-Nilles et al., 2014; Casanova-Nakayama et al., 2011). To predict the potential effect of biomarker modulation on the population of fish, future work should focus on

quantifying those trade-offs, for example by measuring *in vivo* or by searching in the literature the effect of varying immunocompetence in fish on the different biological functions.

Funding information

This work was supported by the French National program EC2CO (Ecosphère Continentale et Côtière) as part of the DERBI project, and by the French Ministry of ecological transition (P190). This project has also received funding from the European Union's Horizon Europe research and innovation programme under Grant Agreement No 101057014 (The European Partnership for the Assessment of Risks from Chemicals; PARC). Special thanks to our modeler colleagues for their valuable comments.

Author contributions

- Corentin Mit: Investigation, Methodology, Software, Formal analysis, Writing - Original Draft, Writing - Review & Editing.
- Anne Bado Nilles: Conceptualization, Investigation, Supervision, Writing - Review & Editing
- Cyril Turiès : Investigation, Resources.
- Gaëlle Daniele: Formal analysis, Investigation, Writing - Review & Editing
- Barbara Giroud: Formal analysis, Investigation, Resources, Writing - Review & Editing
- Rémy Beaudouin: Conceptualization, Investigation, Methodology, Formal analysis, Software, Supervision, Writing - Review & Editing.

5. References

Abbas, R., Hayton, W.L., 1997. A Physiologically Based Pharmacokinetic and Pharmacodynamic Model for Paraoxon in Rainbow Trout. Toxicology and Applied Pharmacology 145, 192-201.

Ankley, G.T., Bennett, R.S., Erickson, R.J., Hoff, D.J., Hornung, M.W., Johnson, R.D., Mount, D.R., Nichols, J.W., Russom, C.L., Schmieder, P.K., Serrrano, J.A., Tietge, J.E., Villeneuve, D.L., 2010. Adverse outcome pathways: A conceptual framework to support ecotoxicology research and risk assessment. Environmental Toxicology and Chemistry 29, 730-741.

Bado-Nilles, A., Techer, R., Porcher, J.M., Geffard, A., Gagnaire, B., Betoulle, S., Sanchez, W., 2014. Detection of immunotoxic effects of estrogenic and androgenic endocrine disrupting compounds using splenic immune cells of the female three-spined stickleback, Gasterosteus aculeatus (L.). Environmental Toxicology and Pharmacology 38, 672-683.

Barber, I., Arnott, S.A., Braithwaite, V.A., Andrew, J., Huntingford, F.A., 2001. Indirect fitness consequences of mate choice in sticklebacks: offspring of brighter males grow slowly but resist parasitic infections. Proceedings. Biological sciences 268, 71-76.

Beausoleil, C., Ormsby, J.-N., Gies, A., Hass, U., Heindel, J.J., Holmer, M.L., Nielsen, P.J., Munn, S., Schoenfelder, G., 2013. Low dose effects and non-monotonic dose responses for endocrine active chemicals: Science to practice workshop: Workshop summary. Chemosphere 93, 847-856.

Bois, F.Y., 2009. GNU MCSim: Bayesian statistical inference for SBML-coded systems biology models. Bioinformatics 25, 1453-1454.

Boucher, J.G., Boudreau, A., Ahmed, S., Atlas, E., 2015. *In Vitro* Effects of Bisphenol A β-D-Glucuronide (BPA-G) on Adipogenesis in Human and Murine Preadipocytes. Environmental Health Perspectives 123, 1287-1293.

Bundgaard, C., Larsen, F., Jørgensen, M., Mørk, A., 2007. Pharmacokinetic/Pharmacodynamic Feedback Modelling of the Functional Corticosterone Response in Rats after Acute Treatment with Escitalopram. Basic & Clinical Pharmacology & Toxicology 100, 182-189.

Casanova-Nakayama, A., Wenger, M., Burki, R., Eppler, E., Krasnov, A., Segner, H., 2011. Endocrine disrupting compounds: Can they target the immune system of fish? Marine Pollution Bulletin 63, 412-416.

Catteau, A., Bado-Nilles, A., Beaudouin, R., Tebby, C., Joachim, S., Palluel, O., Turiès, C., Chrétien, N., Nott, K., Ronkart, S., Geffard, A., Porcher, J.-M., 2021. Water quality of the Meuse watershed: Assessment using a multi-biomarker approach with caged three-spined stickleback (Gasterosteus aculeatus L.). Ecotoxicology and Environmental Safety 208, 111407.

Catteau, A., Le Guernic, A., Marchand, A., Hani, Y.M.I., Palluel, O., Turiès, C., Bado-Nilles, A., Dedourge-Geffard, O., Geffard, A., Porcher, J.-M., 2019. Impact of confinement and food access restriction on the three-spined stickleback (Gasterosteus aculeatus, L.) during caging: a multi-biomarker approach. Fish Physiology and Biochemistry 45, 1261-1276.

Catteau, A., Porcher, J.M., Bado-Nilles, A., Bonnard, I., Bonnard, M., Chaumot, A., David, E., Dedourge-Geffard, O., Delahaut, L., Delorme, N., Francois, A., Garnero, L., Lopes, C., Nott, K., Noury, P., Palluel, O., Palos-Ladeiro, M., Queau, H., Ronkart, S., Sossey-Alaoui, K., Turies, C., Tychon, B., Geffard, O., Geffard, A., 2022. Interest of a multispecies approach in active biomonitoring: Application in the Meuse watershed. Science of the Total Environment 808.

Crain, D.A., Eriksen, M., Iguchi, T., Jobling, S., Laufer, H., LeBlanc, G.A., Guillette, L.J., 2007. An ecological assessment of bisphenol-A: Evidence from comparative biology. Reproductive Toxicology 24, 225-239.

David, V., Joachim, S., Porcher, J.-M., Beaudouin, R., 2019. Modelling BPA effects on three-spined stickleback population dynamics in mesocosms to improve the understanding of population effects. Science of The Total Environment 692, 854-867.

Dayneka, N.L., Garg, V., Jusko, W.J., 1993. Comparison of four basic models of indirect pharmacodynamic responses. Journal of Pharmacokinetics and Biopharmaceutics 21, 457-478.

de Kermoysan, G., Pery, A.R., Porcher, J.M., Beaudouin, R., 2013. A non-invasive method based on head morphology to sex mature three-spined stickleback (*Gasterosteus aculeatus L*.) in rearing conditions. Math Biosci 244, 148-153.

EFSA, 2022. Stakeholder meeting on the draft scientific opinion on re-evaluation of bisphenol A (BPA).

Faheem, M., Adeel, M., Khaliq, S., Lone, K.P., El-Din-H-Sayed, A., 2020. Bisphenol-A induced antioxidants imbalance and cytokines alteration leading to immune suppression during larval development of Labeo rohita. Environmental Science and Pollution Research 27, 26800-26809.

Faheem, M., Bhandari, R.K., 2021. Detrimental Effects of Bisphenol Compounds on Physiology and Reproduction in Fish: A Literature Review. Environ Toxicol Phar 81, 103497.

Felmlee, M.A., Morris, M.E., Mager, D.E., 2012. Mechanism-Based Pharmacodynamic Modeling, in: Reisfeld, B., Mayeno, A.N. (Eds.), Computational Toxicology: Volume I. Humana Press, Totowa, NJ, pp. 583-600.

Filby, A.L., Tyler, C.R., 2005. Molecular Characterization of Estrogen Receptors 1, 2a, and 2b and Their Tissue and Ontogenic Expression Profiles in Fathead Minnow (Pimephales promelas)1. Biology of Reproduction 73, 648-662.

Flint, S., Markle, T., Thompson, S., Wallace, E., 2012. Bisphenol A exposure, effects, and policy: A wildlife perspective. Journal of Environmental Management 104, 19-34.

Forbes, V.E., Palmqvist, A., Bach, L., 2006. The use and misuse of biomarkers in ecotoxicology. Environmental Toxicology and Chemistry 25, 272-280.

Grech, A., Brochot, C., Dorne, J.-L., Quignot, N., Bois, F.Y., Beaudouin, R., 2017. Toxicokinetic models and related tools in environmental risk assessment of chemicals. Science of The Total Environment 578, 1-15.

Harris, J., Bird, D.J., 2000. Modulation of the fish immune system by hormones. Veterinary immunology and immunopathology 77, 163-176.

Lee, J.-H., Landrum, P.F., Koh, C.-h., 2002. Prediction of Time-Dependent PAH Toxicity in Hyalella azteca Using a Damage Assessment Model. Environmental Science & Technology 36, 3131-3138.

Liao, C.-M., Liang, H.-M., Chen, B.-C., Singh, S., Tsai, J.-W., Chou, Y.-H., Lin, W.-T., 2005. Dynamical coupling of PBPK/PD and AUC-based toxicity models for arsenic in tilapia Oreochromis mossambicus from blackfoot disease area in Taiwan. Environmental Pollution 135, 221-233.

Ling, M.P., Liao, C.M., Tsai, J.W., Chen, B.C., 2005. A PBTK/TD Modeling-Based Approach Can Assess Arsenic Bioaccumulation in Farmed Tilapia (Oreochromis mossambicus) and Human Health Risks. Integr. Environ. Assess. Manag. 1, 40-54.

Liu, D., Pan, L., Yang, H., Wang, J., 2014. A physiologically based toxicokinetic and toxicodynamic model links the tissue distribution of benzo[a]pyrene and toxic effects in the scallop Chlamys farreri. Environmental Toxicology and Pharmacology 37, 493-504.

Marchand, A., Porcher, J.-M., Turies, C., Chadili, E., Palluel, O., Baudoin, P., Betoulle, S., Bado-Nilles, A., 2017. Evaluation of chlorpyrifos effects, alone and combined with lipopolysaccharide stress, on DNA integrity and immune responses of the three-spined stickleback, Gasterosteus aculeatus. Ecotoxicology and Environmental Safety 145, 333-339.

Marchand, A., Tebby, C., Beaudouin, R., Hani, Y.M.I., Porcher, J.-M., Turies, C., Bado-Nilles, A., 2019. Modelling the effect of season, sex, and body size on the three-spined stickleback, Gasterosteus aculeatus, cellular innate immunomarkers: A proposition of laboratory reference ranges. Science of The Total Environment 648, 337-349.

Massart, S., Milla, S., Kestemont, P., 2014. Expression of gene, protein and immunohistochemical localization of the estrogen receptor isoform ERα1 in male rainbow trout lymphoid organs; indication of the role of estrogens in the regulation of immune mechanisms. Comparative Biochemistry and Physiology Part B: Biochemistry and Molecular Biology 174, 53-61.

Michałowicz, J., 2014. Bisphenol A – Sources, toxicity and biotransformation. Environmental Toxicology and Pharmacology 37, 738-758.

Milla, S., Depiereux, S., Kestemont, P., 2011. The effects of estrogenic and androgenic endocrine disruptors on the immune system of fish: a review. Ecotoxicology 20, 305-319.

Mit, C., Bado-Nilles, A., Daniele, G., Giroud, B., Vulliet, E., Beaudouin, R., 2022. The toxicokinetics of bisphenol A and its metabolites in fish elucidated by a PBTK model. Aquatic Toxicology 247, 106174.

Mit, C., Tebby, C., Gueganno, T., Bado-Nilles, A., Beaudouin, R., 2021. Modeling acetylcholine esterase inhibition resulting from exposure to a mixture of atrazine and chlorpyrifos using a physiologically-based kinetic model in fish. Science of The Total Environment 773, 144734.

Oliviero, F., Marmugi, A., Viguié, C., Gayrard, V., Picard-Hagen, N., Mselli-Lakhal, L., 2022. Are BPA Substitutes as Obesogenic as BPA? International Journal of Molecular Sciences 23, 4238.

Ougier, E., Zeman, F., Antignac, J.-P., Rousselle, C., Lange, R., Kolossa-Gehring, M., Apel, P., 2021. Human biomonitoring initiative (HBM4EU): Human biomonitoring guidance values (HBM-GVs) derived for bisphenol A. Environment International 154, 106563.

Pandey, M., Ghorai, S.M., Rai, U., 2018. Bisphenol A mediated effects on innate immunity in freshwater teleost spotted snakehead Channa punctatus murrel. Fisheries Science 84, 25-31.

Peillex, C., Kerever, A., Lachhab, A., Pelletier, M., 2021. Bisphenol A, bisphenol S and their glucuronidated metabolites modulate glycolysis and functional responses of human neutrophils. Environ Res 196, 110336.

R Core Team, 2019. R: A Language and Environment for Statistical Computing. R Foundation for Statistical Computing, Vienna, Austria.

Samuel, O.D., Adeyemi, J.A., Bamidele, O.S., Barbosa, F., Adedire, C.O., 2022. Cytotoxicity, redox and immune status in African catfish, Clarias gariepinus (Burchell, 1822) exposed to bisphenol A (BPA) and its analogues. Environmental Science and Pollution Research.

Sheiner, L.B., Stanski, D.R., Vozeh, S., Miller, R.D., Ham, J., 1979. Simultaneous modeling of pharmacokinetics and pharmacodynamics: Application to d-tubocurarine. Clinical Pharmacology & Therapeutics 25, 358-371.

Spromberg, J.A., Meador, J.P., 2006. Relating chronic toxicity responses to population-level effects: A comparison of population-level parameters for three salmon species as a function of low-level toxicity. Ecological Modelling 199, 240-252.

Tao, S., Zhang, Y., Yuan, C., Gao, J., Wu, F., Wang, Z., 2016. Oxidative stress and immunotoxic effects of bisphenol A on the larvae of rare minnow Gobiocypris rarus. Ecotoxicology and Environmental Safety 124, 377-385.

Tebby, C., Brochot, C., Dorne, J.-L., Beaudouin, R., 2019. Investigating the interaction between melamine and cyanuric acid using a Physiologically-Based Toxicokinetic model in rainbow trout. Toxicology and Applied Pharmacology 370, 184-195.

Vandenberg, L.N., Colborn, T., Hayes, T.B., Heindel, J.J., Jacobs, D.R., Lee, D.H., Shioda, T., Soto, A.M., vom Saal, F.S., Welshons, W.V., Zoeller, R.T., Myers, J.P., 2012. Hormones and Endocrine-Disrupting Chemicals: Low-Dose Effects and Nonmonotonic Dose Responses. Endocr. Rev. 33, 378-455.

Yang, M., Qiu, W., Chen, B., Chen, J., Liu, S., Wu, M., Wang, K.-J., 2015. The In Vitro Immune Modulatory Effect of Bisphenol A on Fish Macrophages via Estrogen Receptor α and Nuclear Factor-κB Signaling. Environmental Science & Technology 49, 1888-1895.

Yin, D.-q., Hu, S.-q., Ying, G., Li, W., Liu, S.-s., Zhang, A.-q., 2007. Immunotoxicity of bisphenol A to Carassius auratus lymphocytes and macrophages following in vitro exposure. Journal of environmental sciences 19, 232-237.

Zhang, Y., Feng, J., Gao, Y., Liu, X., Qu, L., Zhu, L., 2019. Physiologically based toxicokinetic and toxicodynamic (PBTK-TD) modelling of Cd and Pb exposure in adult zebrafish Danio rerio: Accumulation and toxicity. Environmental Pollution 249, 959-968.

Supporting information to "PBTK-TD model of the phagocytosis activity in three-spined stickleback exposed to BPA"

Corentin Mit [1,2], Anne Bado-Nilles [2], Cyril Turiès [2], Gaëlle Daniele [3], Barbara Giroud [3] and Rémy Beaudouin[1]*

[1] Experimental Toxicology and Modeling Unit, INERIS, UMR-I 02 SEBIO, Verneuil en Halatte, 65550, France. Tel: +33344618238

[2] Ecotoxicology of substances and fields Unit, INERIS, UMR-I 02 SEBIO, Verneuil en Halatte, 65550, France

[3] Univ Lyon, CNRS, Université Claude Bernard Lyon 1, Institut des Sciences Analytiques, UMR 5280, 5 rue de la Doua, F-69100, Villeurbanne, France

*Corresponding author, e-mail: remy.beaudouin@ineris.fr

Supporting information summary

1. Innate immune biomarkers

Immune parameters were measured using the fish spleen which was pressed against 40 µm sterilized nylon mesh with 5 mL Leibvotitz 15 (L15) medium (Sigma) containing lithium heparin (100 mg/L, Sigma), penicillin (100 mg/L, Sigma), and streptomycin (100 mg/L, Sigma) in order to keep only the leukocytes in suspension (Bado-Nilles et al. 2014). This solution was then stored at -4°C and analysed the following day.

Innate immune biomarkers were measured from the leukocyte suspension using a MacsquantX flow cytometer (Miltenyi Biotec, Bergisch Gladbach, Germany). To compare each sample, the leukocyte concentration was normalized to 10^6 cells/ mL of culture medium.

Leukocyte sub-populations (granulocytes-macrophages), as a % of the total leukocyte population (or number of cells), was identified by their size and complexity using forward scatter (FSC) and size scatter (SSC) parameters.

Cell death was characterized by the percentage of cells in apoptosis and necrosis using a double labelling with Yo-PRO®-1 (Thermo Fisher Scientific, USA, final concentration: 3.14 mg/L) and propidium iodure (Thermo Fisher Scientific, USA, final concentration: 5.01 mg/L) probes to obtain fluorescence of apoptotic (FL1, green fluorescence) and necrotic (FL3, red fluorescence) cells.

Leucocytes respiratory burst was also characterized (Chilmonczyk and Monge (1999)). In short, 2',7'- dichlorodihydrofluorescein diacetate acetyl ester (H2DCF-DA, Thermo Fisher Scientific, USA, final concentration: 29.30 mg/L), a stable non-fluorescent molecule was hydrolysed to dichloro-dihydro-fluorescein diacetate (DCFH) by cytosolic enzymes. DCFH was then oxidized by ROS to the fluorescent dichlorofluorescein (DCF) to quantify unstimulated and cells stimulated by phorbol 12-myristate 13-acetate (PMA, Sigma-Aldrich, USA, final concentration: 9.25 mg/L) in FL1. The index of respiratory burst was determined as the ratio of fluorescence of PMA stimulated cells (H2DCF-DA plus PMA) to that of unstimulated cells (H2DCF-DA).

Lysosomal presence in leukocytes were assessed using acridine orange (AO, Sigma, USA), a lysosomotropic weak base, and fluorescence measurement in FL3 (in MFI, fluorescence unit) (Bado-Nilles et al. 2013).

Finally, phagocytic activity was assessed through two parameters, leukocyte adhesion capacity and internalization efficiency, measured in % of total cells was evaluated with fluorescent microsphere at a concentration of 2.7×10^7 particles/mL (Fluorospheres® carboxylate-modified microsphere, diameter 1 µm, Thermo Fisher Scientific, USA) (Gagnaire et al. 2004). Phagocytic capacity corresponded to the fluorescence of at least one bead and phagocytic efficiency to the fluorescence of at least three beads.

2. Water analysis

Water from aquariums where fish were exposed to BPA was sampled at various times and analyzed. Water from control aquariums was analyzed on the first and last day of exposure (short and long experiments). No BPA or metabolites were detected in control aquariums. Short-term exposure data are presented in table S1 for 10 µg/L nominal concentration and table S2 for 100 µg/L nominal concentration. The limit of quantification (LQ) was estimated to be 0.5, 0.35, and 0.20 ng/mL for BPA, BPA gluc, and BPA sulf. The limit of detection (LD) was estimated to 0.3, 0.1, and 0.15 ng/mL for BPA, BPA gluc, and BPA sulf. Long-term exposure data are presented in table S3 for 100 µg/L nominal concentration of BPA.

Table S1. Measured concentrations in water (nominal concentration 10 µg/L)

	BPA (ng/ml)	**BPA glu (ng/ml)**	**BPA sulf (ng/ml)**
	Female- Male	Female- Male	Female- Male
2h	< LQ - < LQ	nd – nd	nd – nd
4h	< LQ - < LQ	nd – nd	nd – nd
8h	4.5 - 5	nd – nd	nd – nd
24h	2.2 - 5.2	nd – nd	nd – nd
48h	6.1 - 5.7	nd – nd	nd – nd
72h	6.4 - 5.8	nd – nd	nd – nd
168h	4.4 - 4.8	nd – nd	nd – nd

Table S2. Measured concentrations in water (nominal concentration 100 µg/L)

	BPA (ng/ml)	**BPA glu (ng/ml)**	**BPA sulf (ng/ml)**
	Female- Male	Female- Male	Female- Male
2h	17.3 - X	nd – nd	nd – nd
4h	23.1 – 25.4	nd – nd	nd – nd
8h	57.9 – X	nd – nd	nd – nd
24h	65.7 – 59.2	1.3 – 1.1	nd – nd
48h	64.2 – 59.6	1.5 – 1.5	nd – nd
72h	66.8 – 64.7	0.8 – 0.8	nd – nd
168h	70.1 – 65.9	2.3 – 1.4	nd – nd

Table S3. Measured concentrations in water (nominal concentration 100 µg/L)

	BPA (ng/ml)
	Female- Male
Day 1	53.2-57.2
Day 3	53.7-60.2
Day 8	47.2-64.2
Day 15	67.8-49.7
Day 21	49.3-58.6

3. Measured concentrations stickleback organs

The liver, blood, and carcass of the fish were also sampled and analyzed to quantify BPA, BPA gluc, and BPA sulf concentrations. Table S4 and S5 show concentrations in the liver, table S6 and S7 concentrations in blood, and table S8 and S9 concentrations in the dried carcass. A ratio was applied to the concentrations measured in the dried carcass to extrapolate the concentrations in the wet carcass. This ratio is available in Brey et al. (2010). The limit of quantification (LQ) for the liver is estimated to be 10 ng/g for BPA, 3 ng/g for BPA gluc, and 0.1 ng/g for BPA sulf. LQ for blood is estimated to be 10 ng/g for BPA, 5 ng/g for BPA gluc and 0.2 ng/g for BPA sulf. Finally, LQ for carcass is estimated to be 20 ng/g for BPA, 10 ng/g for BPA gluc, and 1 ng/g for BPA sulf.

Table S4. Measured concentrations in female stickleback liver

Sample	**[BPA] (ng/g)**		**[BPA-Sulf] (ng/g)**		**[BPA-Gluc] (ng/g)**	
Nominal concentration	10 µg/L	100 µg/L	10 µg/L	100 µg/L	10 µg/L	100 µg/L
DAY 0.25	11.3	181.8	< LQ	10.1	19.8	1586.1
DAY 1	356.5	2051.6	3.8	34.0	405.3	1557.9
DAY 4	100.4	380.7	1.4	14.8	73.5	1169.5
DAY 7	41.7	928.1	1.0	4.5	152.2	234.4
DAY 8	< LQ	501.1	< LQ	7.7	< LQ	902.1
DAY 14	< LQ	20.2	< LQ	0.1	< LQ	23.4

Table S5. Measured concentrations in male stickleback liver

Sample	[BPA] (ng/g)		[BPA-Sulf] (ng/g)		[BPA-Gluc] (ng/g)	
Nominal concentration	10 µg/L	100 µg/L	10 µg/L	100 µg/L	10 µg/L	100 µg/L
DAY 0.25	41.7	471.5	0.4	24.4	26.1	552.3
DAY 1	14.8	2960.9	0.2	17.6	9.1	542.1
DAY 4	57.7	339.3	1.6	19.7	38.6	1117.7
DAY 7	46.1	427.3	0.2	5.6	14.8	170.7
DAY 8	16.1	22.6	0.8	1.5	21	81.9
DAY 14	< LQ	< LQ	< LQ	< LQ	< LQ	< LQ

Table S6. Measured concentrations in female stickleback blood

Sample	**[BPA] (ng/g)**		**[BPA-Sulf] (ng/g)**		**[BPA-Gluc] (ng/g)**	
Nominal concentration	10 µg/L	100 µg/L	10 µg/L	100 µg/L	10 µg/L	100 µg/L
DAY 0.25	< LQ	46,3	< LQ	3,5	24,2	570,0
DAY 1	13,6	117,6	0,7	6,2	93,7	1968,3
DAY 4	14,9	97,7	0,6	6,4	133,9	1465,0
DAY 7	14,3	87,2	0,5	7,4	102,1	1752,1
DAY 8	< LQ	< LQ	< LQ	0,3	<LQ	119,9
DAY 14	< LQ	< LQ	< LQ	< LQ	< LQ	24,4

Table S7. Measured concentrations in male stickleback blood

Sample	**[BPA] (ng/g)**		**[BPA-Sulf] (ng/g)**		**[BPA-Gluc] (ng/g)**	
Nominal concentration	10 µg/L	100 µg/L	10 µg/L	100 µg/L	10 µg/L	100 µg/L
DAY 0.25	< LQ	122,7	0,2	8.6	32,5	961,7
DAY 1	11,4	Analytical issue	1,5	Analytical issue	91,3	Analytical issue
DAY 4	17,6	84,8	1,0	10,4	155,4	1460,1
DAY 7	9,9	77,4	1,0	9,6	124,4	1478,4
DAY 8	< LQ	< LQ	< LQ	1,2	15,3	218,0
DAY 14	< LQ	< LQ	< LQ	< LQ	< LQ	21,5

Table S8. Measured concentrations in female stickleback dried carcass

Sample	**[BPA] (ng/g)**		**[BPA-Sulf] (ng/g)**		**[BPA-Gluc] (ng/g)**	
Nominal concentration	10 µg/L	100 µg/L	10 µg/L	100 µg/L	10 µg/L	100 µg/L
DAY 0.25	< LQ	313,0	1,1	5,5	32,5	499,8
DAY 1	40,2	2634,1	3,1	63,0	252,9	2134,9
DAY 4	43,9	853,1	1,5	22,0	288,5	1460,8
DAY 7	51,1	369,7	2,5	13,3	194,5	2454,7
DAY 8	< LQ	113,9	< LQ	11,0	35,7	507,9
DAY 14	< LQ	< LQ	< LQ	3,5	23,0	15,7

Table S9. Measured concentrations in male stickleback dried carcass

Sample	**[BPA] (ng/g)**		**[BPA-Sulf] (ng/g)**		**[BPA-Gluc] (ng/g)**	
Nominal concentration	10 µg/L	100 µg/L	10 µg/L	100 µg/L	10 µg/L	100 µg/L
DAY 0.25	< LQ	498,5	< LQ	14,8	60,1	617,6
DAY 1	36,6	1825,8	1	49,0	57,8	3993,4
DAY 4	34,3	1403,5	3,8	35,4	210,6	1253,3
DAY 7	45,2	639,3	2	52,6	82,6	1609,7
DAY 8	< LQ	< LQ	1,3	4,4	51,3	74,3
DAY 14	< LQ	< LQ	< LQ	< LQ	23,2	19,8

4. Simulated concentrations in richly perfused tissues

The PBPK presented in Mit et al., 2022 allowed to predict BPA and BPA metabolites in stickleback organs over time by taking measured water concentrations over time as inputs. Then, the toxicodynamic part of the model took as inputs the concentrations of BPA and BPA metabolites in richly perfused tissues (RPT) (used as a proxy for the spleen where immunomarkers were measured). In Table S10, predicted concentrations in RPT for a male stickleback are presented.

Table S10. Predicted concentrations in male stickleback richly perfused tissues

	[BPA] (ng/g)		**[BPA-Sulf] (ng/g)**		**[BPA-Gluc] (ng/g)**	
Nominal concentration	**10 µg/L**	**100 µg/L**	**10 µg/L**	**100 µg/L**	**10 µg/L**	**100 µg/L**
DAY 0.25	2.32	27.7	0.08	0.93	6.75	73.7
DAY 1	3.93	45.0	0.41	4.68	26.4	297.9
DAY 4	4.40	49.0	0.62	6.65	35.3	378.0
DAY 7	3.70	50.0	0.54	6.93	30.1	391.4
DAY 8	0.19	0.23	0.14	1.48	5.13	49.0
DAY 14	0.19	0.19	0.02	0.02	1.53	1.49

5. Statistical analysis

Prior to modelling, a statistical analysis was performed on each immunomarker response over time. All responses were log-transformed. At each date, a one-way ANOVA followed by a post-hoc Dunnett test was used to determine if a true difference existed between conditions and control. Then, the biomarkers presenting the most consistent response over time were selected to be modelled.

5.1. Leucocyte distribution (Figure 2)

Leucocyte distribution - Multiple Comparisons of Means: Dunnett Contrasts

Time (d)	Short experiment	Time (d)	Long Experiment
Day 0.25	Estimate Std. Error t value Pr(>|t|) BPA10 - Control == 0 -0.11891 0.06825 -1.742 0.154404 BPA100 - Control == 0 -0.28108 0.07120 -3.948 0.000452 ***	Day 7	Estimate Std. Error t value Pr(>|t|) BPA - Control == 0 0.2726 0.1598 1.706 0.2190
Day 1	Estimate Std. Error t value Pr(>|t|) BPA10 - Control == 0 -0.07383 0.07282 -1.014 0.495 BPA100 - Control == 0 0.06044 0.07198 0.840 0.610	Day 14	Estimate Std. Error t value Pr(>|t|) BPA - Control == 0 -0.1393 0.1582 -0.881 0.710
Day 4	Estimate Std. Error t value Pr(>|t|) BPA10 - Control == 0 0.08432 0.07614 1.107 0.441 BPA100 - Control == 0 -0.06028 0.07823 -0.771 0.662	Day 21	Estimate Std. Error t value Pr(>|t|) BPA - Control == 0 -0.01312 0.18422 -0.071 1.000
Day 7	Estimate Std. Error t value Pr(>|t|) BPA10 - Control == 0 -0.14604 0.09822 -1.487 0.2442 BPA100 - Control == 0 -0.22151 0.09950 -2.226 0.0553 .		
Day 8	Estimate Std. Error t value Pr(>|t|) BPA10 - Control == 0 -0.1408 0.1105 -1.274 0.3442 BPA100 - Control == 0 -0.2338 0.1105 -2.115 0.0707 .		
Day 14	Estimate Std. Error t value Pr(>|t|) BPA10 - Control == 0 -0.19619 0.07515 -2.611 0.0218 * BPA100 - Control == 0 -0.17917 0.07613 -2.353 0.0411 *		

Signif. codes: 0 '***' 0.001 '**' 0.01 '*' 0.05 '.' 0.1 ' ' 1 (Adjusted p values reported -- single-step method)

5.2. Cellular mortality (Figure 3)

Cellular mortality - Multiple Comparisons of Means: Dunnett Contrasts

Time (d)	Short experiment	Time (d)	Long Experiment
Day 0.25	Estimate Std. Error t value Pr(>|t|) BPA10 - Control == 0 0.07194 0.16293 0.442 0.870 BPA100 - Control == 0 0.16639 0.16997 0.979 0.523	Day 7	Estimate Std. Error t value Pr(>|t|) BPA - Control == 0 0.2726 0.1598 1.706 0.2190
Day 1	Estimate Std. Error t value Pr(>|t|) BPA10 - Control == 0 0.1547 0.1278 1.210 0.37681 BPA100 - Control == 0 0.3876 0.1263 3.068 0.00631 **	Day 14	Estimate Std. Error t value Pr(>|t|) BPA - Control == 0 -0.1393 0.1582 -0.881 0.710
Day 4	Estimate Std. Error t value Pr(>|t|) BPA10 - Control == 0 0.19547 0.18659 1.048 0.478 BPA100 - Control == 0 -0.07584 0.19171 -0.396 0.894	Day 21	Estimate Std. Error t value Pr(>|t|) BPA - Control == 0 -0.01312 0.18422 -0.071 1.000
Day 7	Estimate Std. Error t value Pr(>|t|) BPA10 - Control == 0 0.21832 0.16991 1.285 0.339 BPA100 - Control == 0 0.09178 0.17213 0.533 0.816		
Day 8	Estimate Std. Error t value Pr(>|t|) BPA10 - Control == 0 0.04079 0.17550 0.232 0.961 BPA100 - Control == 0 0.26845 0.17550 1.530 0.226		
Day 14	Estimate Std. Error t value Pr(>|t|) BPA10 - Control == 0 0.3183 0.1544 2.061 0.0799 . BPA100 - Control == 0 0.3440 0.1565 2.199 0.0588 .		

Signif. codes: 0 '***' 0.001 '**' 0.01 '*' 0.05 '.' 0.1 ' ' 1 (Adjusted p values reported -- single-step method)

5.3. Phagocytic activity (Figure 4)

Splenic immune phagocytosis capacity - Multiple Comparisons of Means: Dunnett Contrasts

Time (d)	Short experiment	Time (d)	Long Experiment
Day 0.25	Estimate Std. Error t value Pr(>|t|) BPA10 - Control == 0 0.03539 0.04533 0.781 0.656 BPA100 - Control == 0 0.01704 0.04729 0.360 0.911	Day 7	Estimate Std. Error t value Pr(>|t|) BPA - Control == 0 0.13222 0.02982 4.434 <1e-04 ***
Day 1	Estimate Std. Error t value Pr(>|t|) BPA10 - Control == 0 0.07160 0.03190 2.245 0.0525 . BPA100 - Control == 0 0.07271 0.03152 2.307 0.0455 *	Day 14	Linear Hypotheses: Estimate Std. Error t value Pr(>|t|) BPA - Control == 0 -0.003677 0.028514 -0.129 0.99847
Day 4	Estimate Std. Error t value Pr(>|t|) BPA10 - Control == 0 -0.009290 0.024258 -0.383 0.899 BPA100 - Control == 0 -0.003981 0.024567 -0.162 0.981	Day 21	Estimate Std. Error t value Pr(>|t|) BPA - Control == 0 -0.03190 0.02810 -1.135 0.531
Day 7	Estimate Std. Error t value Pr(>|t|) BPA10 - Control == 0 0.00671 0.03179 0.211 0.968 BPA100 - Control == 0 0.02656 0.03220 0.825 0.624		
Day 8	Estimate Std. Error t value Pr(>|t|) BPA10 - Control == 0 0.009674 0.022386 0.432 0.8737 BPA100 - Control == 0 0.059799 0.022386 2.671 0.0186 *		
Day 14	Estimate Std. Error t value Pr(>|t|) BPA10 - Control == 0 0.0005394 0.0210658 0.026 1.000 BPA100 - Control == 0 -0.0385426 0.0213411 -1.806 0.135		

Signif. codes: 0 '***' 0.001 '**' 0.01 '*' 0.05 '.' 0.1 ' ' 1 (Adjusted p values reported -- single-step method)

Splenic immune phagocytosis efficiency - Multiple Comparisons of Means: Dunnett Contrasts

Time (d)	Short experiment	Time (d)	Long Experiment
Day 0.25	Estimate Std. Error t value Pr(>|t|) BPA10 - Control == 0 0.11062 0.08295 1.334 0.3162 BPA100 - Control == 0 0.17986 0.08653 2.079 0.0775 .	Day 7	Estimate Std. Error t value Pr(>|t|) BPA - Control == 0 0.35585 0.07569 4.702 < 1e-04 ***
Day 1	Estimate Std. Error t value Pr(>|t|) BPA10 - Control == 0 0.11571 0.08033 1.44 0.26183 BPA100 - Control == 0 0.24052 0.07939 3.03 0.00703 **	Day 14	Estimate Std. Error t value Pr(>|t|) BPA - Control == 0 0.15595 0.08165 1.910 0.148
Day 4	Estimate Std. Error t value Pr(>|t|) BPA10 - Control == 0 0.04458 0.07306 0.610 0.766 BPA100 - Control == 0 0.08891 0.07399 1.202 0.383	Day 21	Estimate Std. Error t value Pr(>|t|) BPA - Control == 0 -0.08321 0.06929 -1.201 0.488
Day 7	Estimate Std. Error t value Pr(>|t|) BPA10 - Control == 0 0.11816 0.05628 2.099 0.0735 . BPA100 - Control == 0 0.29615 0.05702 5.194 5.92e-06 ***		
Day 8	Estimate Std. Error t value Pr(>|t|) BPA10 - Control == 0 0.10013 0.07246 1.382 0.29034 BPA100 - Control == 0 0.30513 0.07246 4.211 0.00018 ***		
Day 14	Estimate Std. Error t value Pr(>|t|) BPA10 - Control == 0 0.08029 0.05256 1.528 0.228 BPA100 - Control == 0 0.04283 0.05324 0.804 0.638		

Signif. codes: 0 '***' 0.001 '**' 0.01 '*' 0.05 '.' 0.1 ' ' 1 (Adjusted p values reported -- single-step method)

5.4. Splenic lysosomal presence (Figure 5)

Splenic lysosomal presence - Multiple Comparisons of Means: Dunnett Contrasts

Time (d)	Short experiment	Time (d)	Long Experiment
Day 0.25	Estimate Std. Error t value Pr(>|t|) BPA10 - Control == 0 0.4305 0.1188 3.623 0.00126 ** BPA100 - Control == 0 0.7662 0.1240 6.181 1.74e-07 ***	Day 7	Estimate Std. Error t value Pr(>|t|) BPA - Control == 0 0.04535 0.05625 0.806 0.75976
Day 1	Estimate Std. Error t value Pr(>|t|) BPA10 - Control == 0 0.008383 0.078878 0.106 0.991634 BPA100 - Control == 0 0.320208 0.077958 4.107 0.000254 ***	Day 14	Estimate Std. Error t value Pr(>|t|) BPA - Control == 0 0.06428 0.11646 0.552 0.90314
Day 4	Estimate Std. Error t value Pr(>|t|) BPA10 - Control == 0 0.02615 0.07975 0.328 0.9253 BPA100 - Control == 0 0.18898 0.08194 2.306 0.0461 *	Day 21	Estimate Std. Error t value Pr(>|t|) BPA - Control == 0 -0.10735 0.06184 -1.736 0.206
Day 7	Estimate Std. Error t value Pr(>|t|) BPA10 - Control == 0 0.2265 0.1103 2.053 0.081310 . BPA100 - Control == 0 0.4487 0.1118 4.014 0.000353 ***		
Day 8	Estimate Std. Error t value Pr(>|t|) BPA10 - Control == 0 0.26226 0.08447 3.105 0.005699 ** BPA100 - Control == 0 0.33995 0.08447 4.025 0.000334 ***		
Day 14	Estimate Std. Error t value Pr(>|t|) BPA10 - Control == 0 0.15117 0.09552 1.583 0.20644 BPA100 - Control == 0 0.35552 0.09677 3.674 0.00105 **		

Signif. codes: 0 '***' 0.001 '**' 0.01 '*' 0.05 '.' 0.1 ' ' 1 (Adjusted p values reported -- single-step method)

5.5. Respiratory burst (Figure 6)

Inactivated ROS level (MFI) - Multiple Comparisons of Means: Dunnett Contrasts

Time (d)	Short experiment	Time (d)	Long Experiment
Day 0.25	Estimate Std. Error t value Pr(>|t|) BPA10 - Control == 0 0.2163 0.2537 0.852 0.607 BPA100 - Control == 0 0.3789 0.2647 1.432 0.270	Day 7	Estimate Std. Error t value Pr(>|t|) BPA - Control == 0 1.0180 0.1384 7.357 1.59e-10 ***
Day 1	Estimate Std. Error t value Pr(>|t|) BPA10 - Control == 0 0.3574 0.1197 2.986 0.00793 ** BPA100 - Control == 0 0.9435 0.1183 7.977 1.5e-10 ***	Day 14	Estimate Std. Error t value Pr(>|t|) BPA - Control == 0 1.5816 0.2341 6.755 <1e-08 ***
Day 4	Estimate Std. Error t value Pr(>|t|) BPA10 - Control == 0 0.1340 0.1189 1.127 0.429 BPA100 - Control == 0 0.6753 0.1222 5.526 1.85e-06 ***	Day 21	Estimate Std. Error t value Pr(>|t|) BPA - Control == 0 0.9139 0.1293 7.068 1.11e-09 ***
Day 7	Estimate Std. Error t value Pr(>|t|) BPA10 - Control == 0 0.6234 0.1813 3.438 0.00216 ** BPA100 - Control == 0 1.3647 0.1790 7.626 6.4e-10 ***		
Day 8	Estimate Std. Error t value Pr(>|t|) BPA10 - Control == 0 0.2383 0.1335 1.785 0.140748 BPA100 - Control == 0 0.5465 0.1335 4.094 0.000266 ***		
Day 14	Estimate Std. Error t value Pr(>|t|) BPA10 - Control == 0 0.8298 0.1560 5.320 3.75e-06 *** BPA100 - Control == 0 1.5300 0.1580 9.683 < 1e-10 ***		

Signif. codes: 0 '***' 0.001 '**' 0.01 '*' 0.05 '.' 0.1 ' ' 1 (Adjusted p values reported -- single-step method)

Respiratory burst index - Multiple Comparisons of Means: Dunnett Contrasts

Time (d)	Short experiment	Time (d)	Long Experiment
Day 0.25	Estimate Std. Error t value Pr(>|t|) BPA10 - Control == 0 0.2977 0.2358 1.263 0.3529 BPA100 - Control == 0 0.6506 0.2460 2.645 0.0202 *	Day 7	Estimate Std. Error t value Pr(>|t|) BPA - Control == 0 -0.56271 0.08483 -6.634 <1e-08 ***
Day 1	Estimate Std. Error t value Pr(>|t|) BPA10 - Control == 0 0.4171 0.1832 2.276 0.0488 * BPA100 - Control == 0 0.3287 0.1811 1.815 0.1319	Day 14	Estimate Std. Error t value Pr(>|t|) BPA - Control == 0 -0.4959 0.2015 -2.461 0.0432 *
Day 4	Estimate Std. Error t value Pr(>|t|) BPA10 - Control == 0 0.5306 0.1168 4.541 6.12e-05 *** BPA100 - Control == 0 0.2281 0.1200 1.900 0.113	Day 21	Estimate Std. Error t value Pr(>|t|) BPA - Control == 0 -0.11213 0.08573 -1.308 0.41964
Day 7	Estimate Std. Error t value Pr(>|t|) BPA10 - Control == 0 -0.5310 0.2150 -2.470 0.031 * BPA100 - Control == 0 -0.2999 0.2122 -1.413 0.276		
Day 8	Estimate Std. Error t value Pr(>|t|) BPA10 - Control == 0 0.4447 0.1106 4.021 0.000339 *** BPA100 - Control == 0 0.4697 0.1106 4.246 0.000160 ***		
Day 14	Estimate Std. Error t value Pr(>|t|) BPA10 - Control == 0 -0.07104 0.12247 -0.580 0.787 BPA100 - Control == 0 -0.14071 0.12407 -1.134 0.424		

Signif. codes: 0 '***' 0.001 '**' 0.01 '*' 0.05 '.' 0.1 ' ' 1 (Adjusted p values reported -- single-step method)

6. MCMC calibration

6.1. Parametrization

Calibration was carried out using GNU MCSim v6.2.0 (Bois 2009). Prior distributions are described in Table 2. Data likelihoods are available in section 7. Model code. MCsim gives the possibility to specify a distribution for the data. The probability of realization of modeled outputs was then described with LogNormal distribution with a variation coefficient which was calibrated to consider inter-individual variability (parameter "sigma" Table S4).

6.2. Calibration results

Parameters were calibrated using Monte Carlo Markov Chains, with three chains of 20 000 iterations each. Convergence was assessed in R 3.6.1 (R Core Team 2019) with the package coda by checking that autocorrelations were low (i.e., that the chains were well mixed), that estimates lay well within the prior boundaries, and that the Gelman-Rubin index was close to 1.

Table S11. Summary of posterior distributions for the estimated parameters of the TD model.

Outputs	Parameters	Prior		Posterior : MPV [IC 95%]	
Lysosomal	K_{in}	Uniform	[0 ; 1000 [	705.5	[508.0 ; 994.4]
presence	K_{out}	Uniform	[0 ; 1000 [	3.32	[2.39 ; 4.68]
	S_max_lyso	N(μ=1 , CV=30 %)	[0 ; + ∞ [	1.81	[0.93 ; 2.59]
	SC_50_lyso	N(μ=0.2 , CV=30 %)	[0 ; + ∞ [	0.216	[0.109 ; 0.316]
	K_tol_lyso	N(μ=0.1 , CV=30 %)	[0 ; + ∞ [	0.105	[0.050 ; 0.163]
	kr_delay	N(μ=1 , CV=30 %)	[0 ; + ∞ [	0.989	[0.422 ; 1.58]
	tau	N(μ=8 , CV=30 %)	[7 ; 13]	7.93	[7.08 ; 12.08]
	Sigma	N(μ=2 , CV=30 %)	[1 ; 10 [	1.16	[1.13 ; 1.37]
Phagocytic	K_{in}	Uniform	[0 ; 1000 [	978.7	[256.5 ; 991.0]
efficiency	K_{out}	Uniform	[0 ; 1000 [	37.42	[9.8 ; 39.8]
	K_tol_phago	N(μ=1 , CV=30 %)	[0 ; 1000 [	0.860	[0.337 ; 1.471]
	S_max_phago	N(μ=0.2 , CV=30 %)	[0 ; + ∞ [	0.277	[0.201 ; 0.36]
	SC_50_phago	N(μ=0.1 , CV=30 %)	[0 ; + ∞ [	0.0983	[0.0399 ; 0.154]
	kr_delay	N(μ=1 , CV=30 %)	[0 ; + ∞ [	1.01	[0.50 ; 1.62]
	tau	N(μ=11 , CV=10 %)	[0 ; 22]	12.3	[9.56 ; 13.3]
	Sigma	N(μ=2 , CV=30 %)	[1 ; 10 [	1.10	[1.1 ; 1.14]
Inactivated ROS	K_{in}	Uniform	[0 ; 1000 [	727.1	[200.4 ; 987.1]
	K_{out}	Uniform	[0 ; 1000 [	65.3	[18.1 ; 100.1]
	S_max_rosb	N(μ=1 , CV=30 %)	[0 ; + ∞ [	1.43	[0.95 ; 1.84]
	SC_50_rosb	N(μ=0.1 , CV=30 %)	[0 ; + ∞ [	0.10	[0.045 ; 0.159]
	kr_delay	N(μ=1 , CV=30 %)	[0 ; + ∞ [	1.05	[0.50 ; 1.58]
	tau	N(μ=2 , CV=10 %)	[0 ; 22 [	2.00	[1.60 ; 2.39]
	Sigma	N(μ=2 , CV=30 %)	[1 ; 10 [	1.43	[1.32 ; 1.92]

- Sigma is the geometric standard deviation (exponential, strictly superior to 1, of the standard deviation in log-space) of the lognormal distribution of the data, given the model

Table S12. Model performances (RMSE, mean fold, BIC) for the phagocytic internalization efficiency by backward selection starting from the model with delay and control loop (Equation 6).

phagocytic internalization efficiency	RMSE	Mean fold	BIC	Equation
Delay and control loop (Equation 6)	0.104	1.079	-34.1	$\frac{dR}{dt} = K_{in}.\left(1 + \frac{S_{max} \times D_{art\ glu}}{SC_{50} + D_{art\ glu}}\right) \times \frac{1}{M} - K_{out} \times R$
without delay (Equation 7)	0.100	1.076	-38.7	$\frac{dR}{dt} = K_{in}.\left(1 + \frac{S_{max} \times C_{art\ glu}}{SC_{50} + C_{art\ glu}}\right) \times \frac{1}{M} - K_{out} \times R$
without control loop	0.128	1.093	-22.0	$\frac{dR}{dt} = K_{in}.\left(1 + \frac{S_{max} \times D_{art\ glu}}{SC_{50} + D_{art\ glu}}\right) - K_{out} \times R$

7. Informatic model code (Mcsim 6.2.0)

7.1. Model file for phagocytosis (efficiency)

```
####Author : Corentin Mit
#================================================
# (I.) Informations
#================================================
################################################
# Model BPA
# Base : Vidal - Grech
# Version: PBTK TD
# Update :  Mechanism-based indirect delayed response (1 parameter) WITH feedback
# Date : 05/09/2022
################################
### Units:
##
# Quantity          microg
# Volumes:          ml
# Time:             day
# Flows:            ml/d
# Concentrations:   microg/ml or microg/g
# Vmax:             microg/d/ ml Liver OR microg/d/ g Liver
# Km:               microg/ml
# Masses:           g
# Lenght:           mm
# Temperature:      Celsius
# Ventilation rate: ml/d
# Density of each tissue is considered equal to 1
################################

#================================================
# (II.) Model variables
#================================================


#============================================
#               States
#============================================

States  = {

      L,                                          # Structural length

      #Q_water,                     # Quantity of BPA in water (microg)
      Q_art,                                      # Quantity of BPA in arterial blood (microg)
      Q_ven,                                      # Quantity  BPA in venous blood (microg)
      Q_viscera,                    #   ...   BPA      in viscera (microg)
      Q_lumen_GIT,                  #   ...   BPA      in lumen (microg)
      Q_gonads,                     #   ...   BPA      in gonads(microg)
      Q_kidney,                     #   ...   BPA      in kidney (microg)
      Q_liver,                      #   ...   BPA      in liver (microg)
      Q_skin,                                     #   ...    BPA      in skin (microg)
      Q_brain,                      #   ...   BPA      in brain (microg)
      Q_fat,                                      #   ...    BPA      in fat (microg)
      Q_pp,                                       #   ...    BPA      in poorly perfused (microg)
      Q_rp,                                       #   ...    BPA      in richly perfused (microg)

      Q_admin_gills,                              #   ...  BPA      entering through gills (microg)
      Q_met,                                       #   ...  BPA      metabolized in total (microg)
      Q_excret_feces,                             #   ...  BPA      fecally excreted (microg)
      Q_excret_gills,                             #   ...  BPA      excreted by gills (microg)
      Q_bile,                                      #   ...  BPA      in billiary vesicule (microg)
      Q_met_liver_gluco,            #   ...  BPA metabolized in BPAg in liver (microg)
      Q_met_liver_sulfo,            #   ...  BPA metabolized in BPAs in liver (microg)
      Q_met_plasma_gluco,           #   ...  BPA metabolized in BPAg in plasma (microg)
      Q_met_plasma_sulfo,           #   ...  BPA metabolized in BPAg in plasma (microg)
      Q_excret,                                    # Total of BPA quantity excreted (microg)

      # Q_water_gluco,              # Quantity of BPA-glucuronide conjugates in water (microg)
      Q_art_gluco,                  #  ...        BPA-glucuronide conjugates in arterial blood (microg
      Q_ven_gluco,                  #  ...        BPA-glucuronide conjugates in venous blood (microg)
      Q_lumen_GIT_gluco,   #  ...       BPA-glucuronide conjugates in lumen (microg))
      Q_liver_gluco,                #  ...        BPA-glucuronide conjugates in liver (microg))
      Q_gonads_gluco,               #  ...        BPA-glucuronide conjugates in gonads (microg))
      Q_rob_gluco,                  #  ...        BPA-glucuronide conjugates in rest of body (microg))
      Q_abdo_cavity_gluco,#  ...       BPA-glucuronide conjugates in kidney and viscera (microg))

      Q_excret_gills_gluco,         #  ...       BPA-glucuronide conjugates excreted by gills (microg)
      Q_excret_feces_gluco,         #  ...       BPA-glucuronide conjugates fecally excreted (microg)
      Q_bile_gluco,                               #  ...       BPA-glucuronide conjugates in billiary vesicule (microg)
      Q_excret_gluco,                             # Total of BPA-glucuronide conjugates quantity excreted (microg)

      #Q_water_sulfo,               # Quantity of BPA-sulfate conjugates in water (microg)
      Q_art_sulfo,                  #  ...        BPA-sulfate conjugates in arterial blood (microg
      Q_ven_sulfo,                  #  ...        BPA-sulfate conjugates in venous blood (microg)
      Q_lumen_GIT_sulfo,   #  ...       BPA-sulfate conjugates in lumen (microg))
      Q_liver_sulfo,                #  ...        BPA-sulfate conjugates in liver (microg))
      Q_gonads_sulfo,               #  ...        BPA-sulfate conjugates in gonads (microg))
      Q_rob_sulfo,                  #  ...        BPA-sulfate conjugates in rest of body (microg))
      Q_abdo_cavity_sulfo,#  ...       BPA-sulfate conjugates in kidney and viscera (microg))

      Q_excret_gills_sulfo,         #  ...       BPA-sulfate conjugates excreted by gills (microg)
      Q_excret_feces_sulfo,         #  ...       BPA-sulfate conjugates fecally excreted (microg)
      Q_bile_sulfo,                               #  ...       BPA-sulfate conjugates in billiary vesicule (microg)
      Q_excret_sulfo,                             # Total of BPA-sulfate conjugates quantity excreted (microg)

      #Toxicodynamics
      Response_phago_percent,       #Phagocytosis response (fraction %)
```

```
        RESPONSE_LYSO,       #LYSOSOMAL PRESENCE RESPONSE (MFI)
        RESPONSE_MACRO_PERCENT,         #GRANULOCYTES-MACROPHAGES RESPONSE (FRACTION %)
        RESPONSE_TBARS,      #TBARS RESPONSE(NMOL MDA/G PROT)
        RESPONSE_ROSA,

        M_TBARS,   #MODERATOR
        M_MACRO,   #MODERATOR
        M_LYSO,
        M_ROSA,
        DELAY,
    };


    #================================================
    #              OUTPUTS
    #================================================

    OUTPUTS = {

        C_ART,               #   ...   BPA      IN ARTERIAL BLOOD (MICROG.ML-1)
        C_BRAIN,   #   ...   BPA      IN BRAIN (MICROG.ML-1)
        C_VEN,               #   ...   BPA      IN VENOUS BLOOD (MICROG.ML-1)
        C_VISCERA, #   ...   BPA      IN VISCERA (MICROG.ML-1)
        C_GONADS,  #   ...   BPA      IN GONADS(MICROG.ML-1)
        C_LIVER,   #   ...   BPA      IN LIVER (MICROG.ML-1)
        C_SKIN,              #   ...   BPA      IN SKIN (MICROG.ML-1)
        C_FAT,               #   ...   BPA      IN FAT (MICROG.ML-1)
        C_PP,                #   ...   BPA      IN PP (MICROG.ML-1)
        C_RP,                #   ...   BPA      IN RP (MICROG.ML-1)
        C_CARCASS, #   ...   BPA      IN CARCASS (MICROG.ML-1)
        C_TOT,               #   ...   BPA      IN TOTAL (MICROG.ML-1)
        C_TOT_BILE, # TOTAL CONCENTRATION IN FISH OF BPA INCLUDING THE QUANTITY IN BILIARY VESICULE (MICROG.ML-1)

        Q_ADMIN_TOT,         #   ...   BPA      ABSORBED IN TOTAL (MICROG)
        Q_ELIM_TOT,                    #   ...   BPA      ELIMINATED IN TOTAL (MICROG)
        Q_BODY,                        # TOTAL OF BPA QUANTITY IN FISH BODY (MICROG)

        # C_WATER_GLUCO,                         # CONCENTRATION OF BPA-GLUCURONIDE CONJUGATES IN WATER (MICROG.ML-1)
        C_ART_GLUCO,                           #       ...        BPA-GLUCURONIDE CONJUGATES IN ARTERIAL BLOOD (MICROG.ML-1)
        C_VEN_GLUCO,                           #       ...        BPA-GLUCURONIDE CONJUGATES IN VENOUS BLOOD (MICROG.ML-1)
        C_GONADS_GLUCO,                        #       ...        BPA-GLUCURONIDE CONJUGATES IN GONADS (MICROG.ML-1)
        C_LIVER_GLUCO,                         #       ...        BPA-GLUCURONIDE CONJUGATES IN LIVER(MICROG.ML-1)
        C_ROB_GLUCO,                           #       ...        BPA-GLUCURONIDE CONJUGATES IN REST OF FISH BODY (MICROG.ML-1)
        C_ABDO_CAVITY_GLUCO, #       ...        BPA-GLUCURONIDE CONJUGATES IN KIDNEY AND VISCERA (MICROG))
        C_TOT_GLUCO,                           # TOTAL CONCENTRATION OF BPA-GLUCURONIDE CONJUGATES IN FISH BODY (MICROG.ML-1)
        C_TOT_BILE_GLUCO,              # TOTAL CONCENTRATION OF BPA-GLUCURONIDE CONJUGATES INCLUDING THE QUANTITY IN BILIARY VESICULE.

        # C_WATER_SULFO,                         # CONCENTRATION OF BPA-SULFATE CONJUGATES IN WATER (MICROG.ML-1)
        C_ART_SULFO,                           #       ...        BPA-SULFATE CONJUGATES IN ARTERIAL BLOOD (MICROG.ML-1)
        C_VEN_SULFO,                           #       ...        BPA-SULFATE CONJUGATES IN VENOUS BLOOD (MICROG.ML-1)
        C_GONADS_SULFO,                        #       ...        BPA-SULFATE CONJUGATES IN GONADS (MICROG.ML-1)
        C_LIVER_SULFO,                         #       ...        BPA-SULFATE CONJUGATES IN LIVER (MICROG.ML-1)
        C_ROB_SULFO,                           # CONCENTRATION OF BPA-SULFATE CONJUGATES IN REST OF FISH BODY (MICROG.ML-1)
        C_ABDO_CAVITY_SULFO, #  ...            BPA-SULFATE CONJUGATES IN KIDNEY AND VISCERA (MICROG))
        C_TOT_SULFO,                           # TOTAL CONCENTRATION OF BPA-SULFATE CONJUGATES IN FISH BODY (MICROG.ML-1)
        C_TOT_BILE_SULFO,              #  TOTAL CONCENTRATION IN FISH OF BPA-SULFATE CONJUGATES INCLUDING THE QUANTITY IN BILIARY
VESICULE.

        #NEEDED TO CALIBRATE EXCRETION IN LINDHOLST 2003
        C_TOT_PC,                      # RATIO OF BPA CONCENTRATION AT TIME T AND AT 7D
        C_TOT_GLUCO_PC,                # RATIO OF BPAG CONCENTRATION AT TIME T AND AT 7D
        C_TOT_SULFO_PC,                # RATIO OF BPAS CONCENTRATION AT TIME T AND AT 7D

        C_TOT_LIND,                            # SAVE CONCENTRATIONS OF BPA AT T = 7D
        C_TOT_GLUCO_LIND,    # SAVE CONCENTRATIONS OF BPAG AT T = 7D
        C_TOT_SULFO_LIND,    # SAVE CONCENTRATIONS OF BPAS AT T = 7D

        # VARIABLES COMPUTED TO EVALUATE THE MODEL
        MASS_BAL,                      # MASS BALANCE (MICROG.ML-1)
        # MASS_BAL_SYS,                # MASS BALANCE INCLUDING QUANTITY IN AQUARIUM (MICROG.ML-1)
        MASS_BAL_GLUCO,                # MASS BALANCE  OF BPA-GLUCURONIDE CONJUGATES(MICROG.ML-1)
        MASS_BAL_SULFO,                # MASS BALANCE OF BPA-SULFATE CONJUGATE(MICROG.ML-1)
        BW,                                    # FISH BODY MASS (G)
        LENGTH,                                # PHYSICAL TOTAL LENGTH (MM)

        #OTHER VARIABLES
        C_BISPHENOL,         # CONCENTRATION OF BISPHENOL ALL FORMS TAKE INTO ACCOUNT.

        #TOXICODYNAMICS
        RATIO_PHAGO_PERCENT, #CALIBRATION
        RATIO_TBARS,
        RATIO_MACRO_PERCENT, #CALIBRATION
        RATIO_LYSO,
        RATIO_ROSA,
        #M_PHAGO, #MODERATOR
        };


    #================================================
    #              INPUTS
    #================================================

    INPUTS  = {
        TEMPERATURE,         # WATER TEMPERATURE EXPRESSED IN DEGREE CELSIUS
        C_WATER,             # CONCENTRATION OF BPA CHEMICAL IN WATER (MICROG.ML-1)
        V_WATER,             # VOLUME OF AQUARIUM (ML)
        BW_I,                          # INITIAL MASS OF FISH (G)
        IVQUANTITY,                    # INTRAVENOUS QUANTITY (µG)
        F_CST,                         # FOOD LEVEL 1 = AD-LIBITUM, 0= STARVATION
        EVENT_BILE};         #<INPUT VARIABLE> = NDOSES(<N>, <LIST-OF-MAGNITUDES>, <LIST-OF-INITIAL-TIMES>);


    #================================================
```

```
# (III) Model parameters
#================================================

        #------------------------------------------------
        # Physiological parameters
        #------------------------------------------------
        Bw_Fcard_ref         ;# Body weight of reference for F_card
        Bw_VO2_ref                    ;# Body weight of reference for VO2 from MacLeod, 1996
        DEB_v                         ;# Energy conductance (mm/d) (DEB model parameter)
        DEB_g                         ;# Energy investment ratio (SU) (DEB model parameter)
        DEB_kM                        ;# Somatic maintenance rate coefficient (1/d) (DEB model parameter)
        DEB_EHm                       ;# Energy at State of maturity at metamorphosis (J)
        DEB_EHb                       ;# Energy at State of maturity at birth (J)
        DEB_shape            ;
        a_BW_L                        ;# a relation BW(g)=F(L(cm))
        b_BW_L                        ;# b relation BW(g)=F(L(cm))

        #------------------------------------------------
        # Environmental condition
        #------------------------------------------------
        TA                                  ;# Arrhenius temperature  in Kelvin
        TR_excretion         ;# Arrhenius reference temperature for the excretion processes (Kelvin)
        TR_DEB                        ;# Arrhenius reference temperature for the DEB model(Kelvin)
        TR_Fcard             ;# Arrhenius reference temperature for cardiac output(Kelvin) -> temperature optimal : 25 C
        TR_VO2                        ;# Arrhenius reference temperature for repsiration(Kelvin)

        #------------------------------------------------
        # Effective respiratory volume & cardiac output
        #------------------------------------------------
        F_card_ref; # Qb_ref_RT * (Bw_ref^(0.75)) / Bw_ref # (ml/d/g) = 28.5 * (7.66^(0.75)) / 7.66 --> allometric scalling
function
        V_O2_ref  ; # reference oxygen comsuption rate (mg/kg/min) --> 2.236044 * 60 * 24 / 1000 mg/g/d from MacLoed, 1966
        O2_EE                ; # Oxygen extraction efficiency of 71% proposed by Erickson, 1990
        Sat                           ; # dissolved oxygen saturation of 90% proposed by Erickson, 1990
        frac_art_ven = (1.0/3.0);  # fraction of arterial blood

        #------------------------------------------------
        # volume scaling factor : fraction of Bw (%)
        #------------------------------------------------
        sc_blood   ;# volume scaling factor, expressed in % Bw (g)
        sc_gonads  ;
        sc_brain   ;
        sc_liver   ;
        sc_fat               ;
        sc_skin              ;
        sc_viscera ;
        sc_kidney  ;
        sc_rp                ;
        sc_pp                ;

        #------------------------------------------------
        # Fraction of arterial blood flow
        #------------------------------------------------
        frac_gonads                   ;# Fraction of arterial blood flow
        frac_brain           ;
        frac_liver           ;
        frac_fat             ;
        frac_skin            ;
        frac_viscera         ;
        frac_kidney                   ;
        frac_rp                       ;
        frac_pp                       ;

        a_Fpp = 0.4                   ;# Fraction of PPT blood going to venous
        a_Fs  = 0.1                   ;# Fraction of skin blood going to venous

        plasma     ;# Plasma fraction 1 - Haematocrit

        #------------------------------------------------
        # Exposure quantity (microg)
        #------------------------------------------------
        WaterQuantity ;
        ivQuantity ;

        #------------------------------------------------
        # Chemical parameters
        #------------------------------------------------
        Unbound_fraction                                ;          # between 0 and 1
        Unbound_fraction_gluco                          ;          # between 0 and 1
        Unbound_fraction_sulfo                          ;          # between 0 and 1

        #------------------------------------------------
        # Partition coefficient  (PC QSAR in .R, need adaptation to organ compositions )
        #------------------------------------------------
        PC_blood_water       ;          # Partition coef blood water for BPA
        PC_liver             ;          # Partition coef liver ""
        PC_gonads            ;          # Partition coef gonade ""
        PC_viscera           ;          # Partition coef viscera ""
        PC_fat                          ;          # Partition coef fat for ""
        PC_kidney            ;          # Partition coef kidney ""
        PC_skin                         ;          # Partition coef skin ""
        PC_brain             ;          # Partition coef brain ""
        PC_rp                           ;          # partition coef rp ""
        PC_pp                           ;          # partition coef pp ""

        #PC_blood_water_gluco           ; # Partition coef blood water for BPA-G
        PC_liver_gluco                  ;
        PC_gonads_gluco                 ;
        PC_abdo_cavity_gluco ;
        PC_rob_gluco                    ;

        #PC_blood_water_sulfo           ; # Partition coef blood water for BPA-S
        PC_liver_sulfo                  ;
```

```
        PC_GONADS_SULFO                         ;
        PC_ABDO_CAVITY_SULFO ;
        PC_ROB_SULFO                            ;

        #-----------------------------------------------
        # METABOLISM   (BASED ON PROT.TOT IN STICKLEBACK)
        #-----------------------------------------------

        KM_GLUCO   ; # MICROG/ML #OHKIMOTO 2003
        VMAX_GLUCO ; # MICROG/D/ML LIVER #OHKIMOTO 2003

        KM_SULFO   ; # MICROG/ML #OHKIMOTO 2003
        VMAX_SULFO ; # MICROG/D/ML LIVER #OHKIMOTO 2003

        #CL_LIVER_GLUCO      ; # ML/D/G LIVER
        #CL_LIVER_SULFO ; # ML/D/G LIVER

        CL_PLASMA_GLUCO      ; # ML/D/ML BLOOD
        CL_PLASMA_SULFO ; # ML/D/ML BLOOD

        #-----------------------------------------------
        # EXCRETION
        #-----------------------------------------------

        K_BG                          ; # EXCRETED FLOW FROM BILLIARY VESICULE TO FAECES (1/D)
        KE_BILE                       ; # EXCRETED FLOW OF BPA FROM LIVER TO BILLIARY VESICULE (1/D)
        KE_BILE_GLUCO        ; # EXCRETED FLOW OF BPA-G FROM LIVER TO BILLIARY VESICULE (1/D)
        KE_BILE_SULFO        ; # EXCRETED FLOW OF BPA-S FROM LIVER TO BILLIARY VESICULE (1/D)

        #-----------------------------------------------
        # FECES AND URINATION
        #-----------------------------------------------
        KE_FECES   = 0.83                       ; # 1/D ESTIMATED FROM NICHOLS  ET AL. 2004
        URINE_RATE = 0.05794769       ; # V_BURST = 1.2 ML.KG-1 EVERY 29.82 MINUTES PROPOSED BY CURTIS 1991 --> 1.2E-03 ML.G BW-
1?

        #-----------------------------------------------
        # TOXICODYNAMIC
        #-----------------------------------------------

        #PHAGOCYTOSIS
        K_IN_PHAGO ;          #FRACTION GAIN*D-1
        K_OUT_PHAGO           ;          #D-1
        S_MAX_PHAGO           ;
        SC_50_PHAGO           ;          #µG/ML
        R0_PHAGO ;
        K_TOL_PHAGO;
        KR_DELAY;
        TAU;
        #MACROPHAGES
        K_IN_MACRO ;          #FRACTION GAIN*D-1
        K_OUT_MACRO           ;          #D-1
        EC_50_MACRO           ;          #µG/ML
        K_TOL_MACRO;
        R0_MACRO ;

        #LYSOSOME
        K_IN_LYSO  ;          #FRACTION GAIN*D-1
        K_OUT_LYSO ;          #D-1
        S_MAX_LYSO ;
        SC_50_LYSO            ;          #µG/ML
        R0_LYSO ;
        K_TOL_LYSO;

        #TBARS
        K_IN_TBARS ;          #FRACTION GAIN*D-1
        K_OUT_TBARS           ;          #D-1
        S_MAX_TBARS           ;
        SC_50_TBARS           ;          #µG/ML
        R0_TBARS ;
        K_TOL_TBARS;
        #ROSA
        K_IN_ROSA  ;          #FRACTION GAIN*D-1
        K_OUT_ROSA ;          #D-1
        S_MAX_ROSA ;
        SC_50_ROSA            ;          #µG/ML
        R0_ROSA ;
        K_TOL_ROSA ;
        # -----------------------------------------------
        # OTHER PARAMETERS THAT WILL BE COMPUTED IN INITIALIZE
        #-----------------------------------------------
        CONV_GLUCO = (404/228.29); # RATIO MOLAR MASS BPA-G/BPA
        CONV_SULFO = (308/228.29); # RATIO MOLAR MASS BPA-S/BPA
        WATER_CONTENT_BLOOD ; # BERTELSEN 1998 IN TROUT
        C_TOT_LIND                              ; #µG/G
        C_TOT_GLUCO_LIND              ; #µG/G
        C_TOT_SULFO_LIND              ; #µG/G
        ABS_EFF                                         ; #GILLS ABSORPTION EFFICIENCY (0-1)
        RATIO_PC_UF;
        RATIO_VMAX_KM_GLUCO;
        RATIO_VMAX_KM_SULFO;
        SIGMA_C_MACRO;
        SIGMA_C_LYSO;
        SIGMA_C_ROSA;
        SIGMA_C_PHAGO;

    #================================================
    # (IV) MODEL INITIALIZATION
    #================================================

    INITIALIZE {

        SC_PP     = (1 - SC_BLOOD - SC_GONADS  - SC_BRAIN  - SC_LIVER - SC_FAT
```

```
                                    - SC_SKIN  - SC_VISCERA - SC_KIDNEY -SC_RP);

      FRAC_PP    = (1 - FRAC_GONADS - FRAC_BRAIN   - FRAC_LIVER   - FRAC_FAT
                                    - FRAC_SKIN   - FRAC_VISCERA -  FRAC_KIDNEY - FRAC_RP);

      Q_VEN = IVQUANTITY;

      L = POW((BW_I/ A_BW_L), (1/B_BW_L)) * DEB_SHAPE * 10;

      PC_BLOOD_WATER = UNBOUND_FRACTION * RATIO_PC_UF ;
      #PC_BLOOD_WATER_GLUCO = UNBOUND_FRACTION_GLUCO * RATIO_PC_UF_GLUCO      ;
      #PC_BLOOD_WATER_SULFO = UNBOUND_FRACTION_SULFO * RATIO_PC_UF_SULFO      ;


      VMAX_GLUCO = KM_GLUCO * RATIO_VMAX_KM_GLUCO ;
      VMAX_SULFO = KM_SULFO * RATIO_VMAX_KM_SULFO ;

      #----------------
      #TOXICODYNAMICS
      #----------------

      #PHAGOCYTOSIS
      RATIO_PHAGO_PERCENT = 1.0;
      RESPONSE_PHAGO_PERCENT = R0_PHAGO ;
      DELAY = 0.0;

      #MACROPHAGES
      M_MACRO = R0_MACRO;
      RATIO_MACRO_PERCENT = 1.0;
      RESPONSE_MACRO_PERCENT = R0_MACRO ;
      K_IN_MACRO = POW(R0_MACRO,2) * K_OUT_MACRO          ;

      #LYSOSOMES
      M_LYSO = R0_LYSO;
      RATIO_LYSO = 1.0;
      RESPONSE_LYSO = R0_LYSO ;
      K_IN_LYSO = R0_LYSO * K_OUT_LYSO          ;

      #TBARS
      M_TBARS = R0_TBARS;
      RATIO_TBARS = 1.0;
      RESPONSE_TBARS = R0_TBARS ;
      K_IN_TBARS = POW(R0_TBARS,2) * K_OUT_TBARS                    ;

      #ROS A
      M_ROSA = R0_ROSA;
      RATIO_ROSA = 1.0;
      RESPONSE_ROSA = R0_ROSA ;
      K_IN_ROSA = POW(R0_ROSA,2) * K_OUT_ROSA   ;

} # END OF INITIALIZE

#================================================
# (V) ODE EQUATIONS
#================================================

DYNAMICS {

      #SET TEMPERATURE
      TC_K = TEMPERATURE + 273.15; # (DEGREE K)
      TC_C = TEMPERATURE;          # (DEGREE C)

      # BODY WEIGHT : DEB GROWTH MODEL ANISOMORPHIC
      KT_ARRHENIUS          = EXP((TA / TR_DEB) - (TA / TC_K));
      DEB_V_T                       = DEB_V  * KT_ARRHENIUS ;
                                      # MM/D
      DEB_LM                        = DEB_V / (DEB_KM * DEB_G);
                                      # MM
      DEB_M                         = POW((DEB_EHM / DEB_EHB),(1.0/3.0));
                          # EHM AND EHB = J



      DT(L)                         = (DEB_V_T / (3 * (F_CST + DEB_G))) * (F_CST * DEB_M - (L/DEB_LM));
      BW                                  = A_BW_L * POW(( (L/10)/DEB_SHAPE ),(B_BW_L));
                          # BW = G; A = G/CM;  L = MM --> /10 = CM

      #VOLUMES (ML OR G) OF THE ORGANS CHANGING WITH THE TIME
      V_ART                 = SC_BLOOD * BW  * FRAC_ART_VEN * PLASMA; #BPA IN PLASMA FRACTION
      V_VEN                 = SC_BLOOD * BW  * (1-FRAC_ART_VEN) * PLASMA; #BPA IN PLASMA FRACTION

      V_LIVER               = SC_LIVER * BW;
      V_GONADS   = SC_GONADS * BW;
      V_VISCERA  = SC_VISCERA * BW;
      V_KIDNEY   = SC_KIDNEY * BW;
      V_SKIN                = SC_SKIN * BW;
      V_BRAIN               = SC_BRAIN * BW;
      V_FAT                 = SC_FAT * BW;
      V_RP                  = SC_RP * BW;
      V_PP                  = SC_PP * BW;

      # BLOOD FLOW (ML/D)
      F_CARD_G = F_CARD_REF * EXP((TA / TR_FCARD) - (TA / TC_K))  * POW((BW/BW_FCARD_REF),(-0.1)) ;   # CARDIAC OUTPUT = ML/D/G
      F_CARD   = F_CARD_G * BW * PLASMA;   # ML/D OF PLASMA FLOW

      # FLOWS TO TISSUES CORRECTED WITH THE UF
      F_LIVER               = FRAC_LIVER * F_CARD * UNBOUND_FRACTION;
      F_GONADS   = FRAC_GONADS * F_CARD * UNBOUND_FRACTION;
      F_VISCERA  = FRAC_VISCERA * F_CARD * UNBOUND_FRACTION;
      F_KIDNEY   = FRAC_KIDNEY * F_CARD * UNBOUND_FRACTION;
      F_SKIN                = FRAC_SKIN * F_CARD * UNBOUND_FRACTION;
      F_FAT                 = FRAC_FAT * F_CARD * UNBOUND_FRACTION;
      F_BRAIN               = FRAC_BRAIN * F_CARD * UNBOUND_FRACTION;
```

```
          F_RP                = FRAC_RP * F_CARD * UNBOUND_FRACTION;
          F_PP                = FRAC_PP * F_CARD * UNBOUND_FRACTION;

          F_LIVER_GLUCO                 = FRAC_LIVER  * F_CARD * UNBOUND_FRACTION_GLUCO;
          F_GONADS_GLUCO                = FRAC_GONADS * F_CARD * UNBOUND_FRACTION_GLUCO;
          F_ABDO_CAVITY_GLUCO  = (FRAC_KIDNEY + FRAC_VISCERA) * F_CARD * UNBOUND_FRACTION_GLUCO;
          F_ROB_GLUCO                   =    (1-(FRAC_LIVER    +    FRAC_KIDNEY    +    FRAC_GONADS    +    FRAC_VISCERA))*    F_CARD    *
UNBOUND_FRACTION_GLUCO;

          F_LIVER_SULFO                 = FRAC_LIVER  * F_CARD * UNBOUND_FRACTION_SULFO;
          F_GONADS_SULFO                = FRAC_GONADS * F_CARD * UNBOUND_FRACTION_SULFO;
          F_ABDO_CAVITY_SULFO  = (FRAC_KIDNEY + FRAC_VISCERA) * F_CARD * UNBOUND_FRACTION_SULFO;
          F_ROB_SULFO                   = (1-(FRAC_LIVER+ FRAC_KIDNEY + FRAC_GONADS + FRAC_VISCERA))* F_CARD * UNBOUND_FRACTION_SULFO;

          # EFFECTIVE RESPIRATORY VOLUME (ML/D)
          V_O2_G              = V_O2_REF * EXP((TA / TR_VO2) - (TA / TC_K))  * POW((BW/BW_VO2_REF),-0.1) ;            #MG
O2/D/G
          V_O2                = V_O2_G * BW ;                                                                          #     MG
O2/D
          C_O2_WATER          = ((-0.24 * TC_C + 14.04) * SAT )/1000 ;         # MG O2/ML
          F_WATER             = V_O2/ (O2_EE * C_O2_WATER) ;                                    # ML/D
          KX = F_WATER ; #KX = (TMP < F_WATER ? TMP : F_WATER) ;

          ############### BPA CONCENTRATIONS IN TISSUES (MICROG/G = MICROG/ML) ########################
          C_ART               = Q_ART             / V_ART;
          C_VEN               = Q_VEN             / V_VEN;
          C_LIVER             = Q_LIVER  / V_LIVER;
          C_GONADS   = Q_GONADS / V_GONADS;
          C_VISCERA  = Q_VISCERA          / V_VISCERA;
          C_KIDNEY   = Q_KIDNEY / V_KIDNEY;
          C_FAT               = Q_FAT             / V_FAT;
          C_BRAIN             = Q_BRAIN  / V_BRAIN;
          C_SKIN              = Q_SKIN   / V_SKIN;
          C_RP                = Q_RP              / V_RP;
          C_PP                = Q_PP              / V_PP;

          C_TOT               = ((Q_ART + Q_VEN + Q_LIVER + Q_GONADS + Q_SKIN + Q_VISCERA + Q_KIDNEY + Q_BRAIN + Q_FAT + Q_RP +
Q_PP)
                                                                  / (V_ART + V_VEN + V_LIVER + V_GONADS + V_SKIN + V_VISCERA + V_KIDNEY
+ V_BRAIN + V_FAT + V_RP + V_PP));

          C_TOT_BILE= C_TOT + (Q_BILE/BW); # C_TOT_BILE WITH/WITHOUT Q_BILE/BW

          C_CARCASS           = ( Q_SKIN + Q_BRAIN + Q_FAT + Q_RP + Q_PP) / (V_SKIN + V_BRAIN + V_FAT + V_RP + V_PP);


          ############ BPA-G CONCENTRATIONS IN TISSUES (MICROG/G = MICROG/ML) ############################
          C_ART_GLUCO                               = Q_ART_GLUCO    / V_ART;
          C_VEN_GLUCO                               = Q_VEN_GLUCO    / V_VEN;
          C_LIVER_GLUCO                 = Q_LIVER_GLUCO  / V_LIVER;
          C_ABDO_CAVITY_GLUCO  = Q_ABDO_CAVITY_GLUCO/ (V_VISCERA + V_KIDNEY);
          C_GONADS_GLUCO                = Q_GONADS_GLUCO / V_GONADS ;
          C_ROB_GLUCO                               = Q_ROB_GLUCO / (V_SKIN + V_BRAIN + V_FAT + V_RP + V_PP);
          C_TOT_GLUCO                               = ((Q_LIVER_GLUCO + Q_ART_GLUCO + Q_VEN_GLUCO + Q_ROB_GLUCO + Q_ABDO_CAVITY_GLUCO
+ Q_GONADS_GLUCO)
                                                                                    / (V_ART + V_VEN + V_LIVER + V_GONADS + V_SKIN +
V_VISCERA + V_KIDNEY + V_BRAIN + V_FAT + V_RP + V_PP));
          C_TOT_BILE_GLUCO    = C_TOT_GLUCO + (Q_BILE_GLUCO/BW);

          ########## BPA-S CONCENTRATIONS IN TISSUES (MICROG/G = MICROG/ML) ############################
          C_ART_SULFO                               = Q_ART_SULFO    / V_ART;
          C_VEN_SULFO                               = Q_VEN_SULFO    / V_VEN;
          C_LIVER_SULFO                 = Q_LIVER_SULFO  / V_LIVER;
          C_ABDO_CAVITY_SULFO  = Q_ABDO_CAVITY_SULFO/ (V_VISCERA + V_KIDNEY);
          C_GONADS_SULFO                = Q_GONADS_SULFO / V_GONADS ;
          C_ROB_SULFO                               = Q_ROB_SULFO / ( V_SKIN  + V_BRAIN + V_FAT + V_RP + V_PP);
          C_TOT_SULFO                               = ((Q_LIVER_SULFO + Q_ART_SULFO + Q_VEN_SULFO + Q_ROB_SULFO + Q_ABDO_CAVITY_SULFO
+ Q_GONADS_SULFO )
                                                                                    / (V_ART + V_VEN + V_LIVER + V_GONADS + V_SKIN +
V_VISCERA + V_KIDNEY + V_BRAIN + V_FAT + V_RP + V_PP));
          C_TOT_BILE_SULFO    = C_TOT_SULFO + (Q_BILE_SULFO/BW);

          ######## BPA AND METABOLITE CONCENTRATION IN THE WATER : EXPOSURE --> MICROG/G = MICROG/ML ####################
          # C_WATER                     = Q_WATER / V_WATER;
          # C_WATER_GLUCO       = Q_WATER_GLUCO / V_WATER;
          # C_WATER_SULFO       = Q_WATER_SULFO / V_WATER;

          ####### SCALING CLEARANCE AND EXCRETION CONSTANT#####################################
          #SCALING CL TO BLOOD VOLUME
          CL_SC_PLASMA_GLUCO = CL_PLASMA_GLUCO * V_VEN * UNBOUND_FRACTION ;
          CL_SC_PLASMA_SULFO = CL_PLASMA_SULFO * V_VEN * UNBOUND_FRACTION ;


          #SCALING VMAX/CL TO LIVER VOLUME
          VMAX_SC_GLUCO         = VMAX_GLUCO * V_LIVER;
          VMAX_SC_SULFO         = VMAX_SULFO * V_LIVER;
          #CL_SC_LIVER_GLUCO    = CL_LIVER_GLUCO * V_LIVER;
          #CL_SC_LIVER_SULFO    = CL_LIVER_SULFO * V_LIVER;

        #TEMPERATURE CORRECTION
        KE_FECES_T              = KE_FECES * EXP((TA / TR_EXCRETION) - (TA / TC_K));
          KE_BILE_T             = KE_BILE * EXP((TA / TR_EXCRETION) - (TA / TC_K));
          KE_BILE_GLUCO_T       = KE_BILE_GLUCO * EXP((TA / TR_EXCRETION) - (TA / TC_K));
          KE_BILE_SULFO_T       = KE_BILE_SULFO * EXP((TA / TR_EXCRETION) - (TA / TC_K));

          ##### BPA METABOLISM  ###########################################################################

          #BPA TO BPA-G
          DT(Q_MET_LIVER_GLUCO)     = (VMAX_SC_GLUCO *(C_LIVER/PC_LIVER) )/(KM_GLUCO + (C_LIVER/PC_LIVER)) ;
          DT(Q_MET_PLASMA_GLUCO)            = CL_SC_PLASMA_GLUCO * C_VEN ;
          #DT(Q_MET_LIVER_GLUCO)     = CL_SC_LIVER_GLUCO * (C_LIVER/PC_LIVER);

          #BPA TO BPA-S
```

```
          DT(Q_MET_LIVER_SULFO)    = (VMAX_SC_SULFO *(C_LIVER/PC_LIVER) )/(KM_SULFO + (C_LIVER/PC_LIVER)) ;
          DT(Q_MET_PLASMA_SULFO)          = CL_SC_PLASMA_SULFO * C_VEN ;
          #DT(Q_MET_LIVER_SULFO)    = CL_SC_LIVER_GLUCO * (C_LIVER/PC_LIVER);

          #BPA TOTAL METABOLIZED
          DT(Q_MET) = DT(Q_MET_LIVER_GLUCO) + DT(Q_MET_PLASMA_GLUCO) + DT(Q_MET_PLASMA_SULFO) + DT(Q_MET_LIVER_SULFO);

          ######## BPA EXCRETION ##############################################################################
          DT(Q_BILE)= (KE_BILE_T * Q_LIVER * UNBOUND_FRACTION) - EVENT_BILE * K_BG * Q_BILE ;

          DT(Q_EXCRET_GILLS)   = KX * (UNBOUND_FRACTION * C_VEN / PC_BLOOD_WATER);#FIXED TO 0 IN MODEL 1 AND 2
          DT(Q_LUMEN_GIT)              = ( - Q_LUMEN_GIT * KE_FECES_T + EVENT_BILE * K_BG * Q_BILE );
          DT(Q_EXCRET_FECES)   = Q_LUMEN_GIT * KE_FECES_T;
          DT(Q_EXCRET)                 = DT(Q_EXCRET_FECES) + DT(Q_EXCRET_GILLS) ;

          ######## BPA-G EXCRETION ############################################################################
          DT(Q_BILE_GLUCO)                        = (KE_BILE_GLUCO_T * Q_LIVER_GLUCO * UNBOUND_FRACTION_GLUCO) - EVENT_BILE * K_BG
* Q_BILE_GLUCO ;

          DT(Q_LUMEN_GIT_GLUCO)                   = ( - Q_LUMEN_GIT_GLUCO * KE_FECES_T + EVENT_BILE * K_BG * Q_BILE_GLUCO );
          DT(Q_EXCRET_FECES_GLUCO)        = Q_LUMEN_GIT_GLUCO * KE_FECES_T;
          DT(Q_EXCRET_GILLS_GLUCO)        = 0.0; #FIXED TO 0 IN MODEL 1
          DT(Q_EXCRET_GLUCO)                      = DT(Q_EXCRET_FECES_GLUCO)+ DT(Q_EXCRET_GILLS_GLUCO) ;

          ######## BPA-S EXCRETION ############################################################################
          DT(Q_BILE_SULFO)                        = (KE_BILE_SULFO_T * Q_LIVER_SULFO * UNBOUND_FRACTION_SULFO) - EVENT_BILE * K_BG
* Q_BILE_SULFO;

          DT(Q_LUMEN_GIT_SULFO)                   = ( - Q_LUMEN_GIT_SULFO * KE_FECES_T + EVENT_BILE * K_BG * Q_BILE_SULFO );
          DT(Q_EXCRET_FECES_SULFO)        = Q_LUMEN_GIT_SULFO *KE_FECES_T;
          DT(Q_EXCRET_GILLS_SULFO)        = 0.0;#FIXED TO 0 IN MODEL 1
          DT(Q_EXCRET_SULFO)                      = DT(Q_EXCRET_FECES_SULFO)+ DT(Q_EXCRET_GILLS_SULFO) ;

          ########################## BPA ABSORBED : DIFFERENTIALS IN MICROG/D ########################
          DT(Q_ADMIN_GILLS)  = ABS_EFF * KX * C_WATER;         ###GILLS

          ######################################## BPA BLOOD QUANTITY ################################################

          DT(Q_ART) = (F_CARD * C_VEN * UNBOUND_FRACTION
                                                  - F_LIVER * C_ART
                                                  - F_KIDNEY * C_ART
                                                  - F_VISCERA * C_ART
                                                  - F_GONADS * C_ART
                                                  - F_SKIN * C_ART
                                                  - F_FAT * C_ART
                                                  - F_BRAIN * C_ART
                                                  - F_RP * C_ART
                                                  - F_PP * C_ART);

          DT(Q_VEN) = (F_BRAIN * C_BRAIN/PC_BRAIN
                                                   + (F_LIVER + F_GONADS + F_VISCERA + F_RP) * C_LIVER/PC_LIVER
                                                   + F_FAT * C_FAT/PC_FAT
                                                   + (F_KIDNEY + ((1 - A_FPP) * F_PP)
                                                   + ((1 - A_FS) * F_SKIN)) * (C_KIDNEY / PC_KIDNEY)
                                                   + A_FPP * F_PP  * (C_PP / PC_PP)
                                                   + A_FS * F_SKIN * (C_SKIN / PC_SKIN)
                                                   - F_CARD * C_VEN * UNBOUND_FRACTION
                                                   + DT(Q_ADMIN_GILLS)
                                                   - DT(Q_EXCRET_GILLS)
                                                   - DT(Q_MET_PLASMA_GLUCO)
                                                   - DT(Q_MET_PLASMA_SULFO));

          ########################## BPA QUANTITY IN TISSUES ########################################

          DT(Q_GONADS)          = F_GONADS * (C_ART - C_GONADS/PC_GONADS)           ;
          DT(Q_SKIN)            = F_SKIN   * (C_ART - C_SKIN  /PC_SKIN)             ;
          DT(Q_FAT)             = F_FAT    * (C_ART - C_FAT   /PC_FAT)              ;
          DT(Q_RP)              = F_RP     * (C_ART - C_RP    /PC_RP)               ;
          DT(Q_PP)              = F_PP     * (C_ART - C_PP    /PC_PP)               ;
          DT(Q_BRAIN)                   = F_BRAIN  * (C_ART - C_BRAIN /PC_BRAIN) ;

          DT(Q_LIVER)                   = ( F_LIVER * C_ART
                                                  + F_RP *(C_RP /PC_RP )
                                                  + F_VISCERA *(C_VISCERA /PC_VISCERA )
                                                  + F_GONADS *(C_GONADS /PC_GONADS )
                                                  - ( F_LIVER + F_RP + F_VISCERA + F_GONADS  ) *(C_LIVER /PC_LIVER )
                                                  - KE_BILE_T * Q_LIVER * UNBOUND_FRACTION
                                                  - DT(Q_MET_LIVER_GLUCO)
                                                  - DT(Q_MET_LIVER_SULFO));

          DT(Q_KIDNEY)          = ( F_KIDNEY * C_ART
                                                  + (1-A_FPP) * F_PP * (C_PP  / PC_PP )
                                                  + (1-A_FS) * F_SKIN * (C_SKIN  / PC_SKIN )
                                                  - (F_KIDNEY + (1-A_FPP) * F_PP + (1-A_FS) * F_SKIN) * (C_KIDNEY  /
PC_KIDNEY ));

          DT(Q_VISCERA)         = F_VISCERA*(C_ART - C_VISCERA /PC_VISCERA );

          ########################## BPA-G QUANTITY IN TISSUES ########################################

          DT(Q_ART_GLUCO)       =  ( F_CARD * C_VEN_GLUCO * UNBOUND_FRACTION_GLUCO - F_LIVER_GLUCO * C_ART_GLUCO - F_ROB_GLUCO *
C_ART_GLUCO - F_GONADS_GLUCO * C_ART_GLUCO - F_ABDO_CAVITY_GLUCO * C_ART_GLUCO);

          DT(Q_VEN_GLUCO)       = ((F_LIVER_GLUCO + F_GONADS_GLUCO) * (C_LIVER_GLUCO/PC_LIVER_GLUCO))
                                                   + (F_ROB_GLUCO * (C_ROB_GLUCO/PC_ROB_GLUCO))
                                                   + (F_ABDO_CAVITY_GLUCO * (C_ABDO_CAVITY_GLUCO/PC_ABDO_CAVITY_GLUCO))
                                                   - F_CARD * C_VEN_GLUCO * UNBOUND_FRACTION_GLUCO
                                                   - DT(Q_EXCRET_GILLS_GLUCO)
                                                   + (CONV_GLUCO * DT(Q_MET_PLASMA_GLUCO));

          DT(Q_LIVER_GLUCO) = (DT(Q_MET_LIVER_GLUCO) * CONV_GLUCO)
                                                  + F_LIVER_GLUCO * C_ART_GLUCO
                                                  + F_GONADS_GLUCO *(C_GONADS_GLUCO /PC_GONADS_GLUCO )
```

```
                                                    - (F_LIVER_GLUCO + F_GONADS_GLUCO) *(C_LIVER_GLUCO /PC_LIVER_GLUCO )
                                                    - KE_BILE_GLUCO_T * Q_LIVER_GLUCO * UNBOUND_FRACTION_GLUCO;

        DT(Q_ROB_GLUCO)                 = F_ROB_GLUCO * (C_ART_GLUCO - (C_ROB_GLUCO/PC_ROB_GLUCO));
        DT(Q_GONADS_GLUCO)              = F_GONADS_GLUCO * (C_ART_GLUCO - (C_GONADS_GLUCO/PC_GONADS_GLUCO));
        DT(Q_ABDO_CAVITY_GLUCO)         = F_ABDO_CAVITY_GLUCO * (C_ART_GLUCO - (C_ABDO_CAVITY_GLUCO/PC_ABDO_CAVITY_GLUCO));

        ########################### BPA-S QUANTITY  IN TISSUES ######################################

        DT(Q_ART_SULFO)      =  ( F_CARD * C_VEN_SULFO * UNBOUND_FRACTION_SULFO - F_LIVER_SULFO   * C_ART_SULFO - F_ROB_SULFO
*C_ART_SULFO - F_ABDO_CAVITY_SULFO * C_ART_SULFO - F_GONADS_SULFO * C_ART_SULFO);

        DT(Q_VEN_SULFO)      = ((F_LIVER_SULFO + F_GONADS_SULFO) * (C_LIVER_SULFO/PC_LIVER_SULFO))
                                                    + (F_ROB_SULFO * (C_ROB_SULFO/PC_ROB_SULFO))
                                                    + (F_ABDO_CAVITY_SULFO * (C_ABDO_CAVITY_SULFO/PC_ABDO_CAVITY_SULFO))
                                                    - F_CARD * C_VEN_SULFO * UNBOUND_FRACTION_SULFO
                                                    - DT(Q_EXCRET_GILLS_SULFO)
                                                    + (CONV_SULFO * DT(Q_MET_PLASMA_SULFO));

        DT(Q_LIVER_SULFO)  = (DT(Q_MET_LIVER_SULFO) * CONV_SULFO)
                                                    + F_LIVER_SULFO * C_ART_SULFO
                                                    + F_GONADS_SULFO *(C_GONADS_SULFO /PC_GONADS_SULFO )
                                                    - (F_LIVER_SULFO +F_GONADS_SULFO) *(C_LIVER_SULFO /PC_LIVER_SULFO )
                                                    - KE_BILE_SULFO_T * Q_LIVER_SULFO * UNBOUND_FRACTION_SULFO;

        DT(Q_ROB_SULFO)                 = F_ROB_SULFO * (C_ART_SULFO - (C_ROB_SULFO/PC_ROB_SULFO));
        DT(Q_GONADS_SULFO)              = F_GONADS_SULFO *(C_ART_SULFO - (C_GONADS_SULFO/PC_GONADS_SULFO));
        DT(Q_ABDO_CAVITY_SULFO)         = F_ABDO_CAVITY_SULFO * (C_ART_SULFO - (C_ABDO_CAVITY_SULFO/PC_ABDO_CAVITY_SULFO));

        ########################### CHEMICAL KINETIC IN  AQUARIUM WATER ##################################
        #DT(Q_WATER) = (DT(Q_EXCRET) - DT(Q_ELIM_WATER) - DT(Q_ADMIN_GILLS));
        #DT(Q_ELIM_WATER) = KE_WATER * Q_WATER ;
        #DT(Q_WATER_GLUCO) = DT(Q_EXCRET_GLUCO) ;
        #DT(Q_WATER_SULFO) = DT(Q_EXCRET_SULFO) ;

        ########################### SAVE CONCENTRATIONS OF BPA, BPAG AND BPAS AT T = 7D #################
        C_TOT_LIND =  (T == 7 ? C_TOT_BILE : C_TOT_LIND);
        C_TOT_GLUCO_LIND = (T == 7 ? C_TOT_BILE_GLUCO : C_TOT_GLUCO_LIND);
        C_TOT_SULFO_LIND = (T == 7 ? C_TOT_BILE_SULFO : C_TOT_SULFO_LIND);

        ########################### TOXICODYNAMIC PART :  ##################

        M_PHAGO = ( (T -TAU) <1E-12 ? 1 : (1 + (T - TAU) * K_TOL_PHAGO)) ;
        REGULATION =  (DELAY >1E-10? ((1/M_PHAGO)*( S_MAX_PHAGO * DELAY))/(SC_50_PHAGO + DELAY) : 0);
        DT(RESPONSE_PHAGO_PERCENT) = K_IN_PHAGO*(1+ REGULATION) - K_OUT_PHAGO*RESPONSE_PHAGO_PERCENT;
        DT(DELAY) = KR_DELAY*(C_ART_GLUCO -DELAY);


        DT(RESPONSE_MACRO_PERCENT) = K_IN_MACRO*(1- (C_RP/(EC_50_MACRO + C_RP))) - (K_OUT_MACRO/M_MACRO)*RESPONSE_MACRO_PERCENT;

        DT(M_MACRO) = K_TOL_MACRO * RESPONSE_MACRO_PERCENT - K_TOL_MACRO *       M_MACRO;

        DT(RESPONSE_LYSO) = (K_IN_LYSO/M_LYSO)*(1+ (S_MAX_LYSO * C_RP)/(SC_50_LYSO + C_RP)) - K_OUT_LYSO*RESPONSE_LYSO;

        DT(M_LYSO) = K_TOL_LYSO * RESPONSE_LYSO - K_TOL_LYSO *        M_LYSO;

        DT(RESPONSE_TBARS)  =  K_IN_TBARS  -  (K_OUT_TBARS/M_TBARS)*RESPONSE_TBARS*(1+  (S_MAX_TBARS  *  C_LIVER)/(SC_50_TBARS  +
C_LIVER));
        DT(M_TBARS) = K_TOL_TBARS * RESPONSE_TBARS - K_TOL_TBARS *    M_TBARS;

        DT(RESPONSE_ROSA) = K_IN_ROSA*(1+ (S_MAX_ROSA * C_RP)/(SC_50_ROSA + C_RP)) - K_OUT_ROSA*RESPONSE_ROSA;



        DT(M_ROSA) = K_TOL_ROSA * RESPONSE_ROSA - K_TOL_ROSA *        M_ROSA;
    } # END OF DYNAMICS


    CALCOUTPUTS{


        #CALIBRATION WITH LOG(PREDICTION)
        C_TOT                                   = (C_TOT < 0 ? 1E-12 : C_TOT);
        C_TOT_BILE                      = (C_TOT_BILE < 0 ? 1E-12 : C_TOT_BILE);

        C_TOT_GLUCO                             = (C_TOT_GLUCO < 0 ? 1E-12 : C_TOT_GLUCO);
        C_TOT_BILE_GLUCO     = (C_TOT_BILE_GLUCO < 0 ? 1E-12 : C_TOT_BILE_GLUCO);

        C_TOT_SULFO                             = (C_TOT_SULFO < 0 ? 1E-12 : C_TOT_SULFO);
        C_TOT_BILE_SULFO     = (C_TOT_BILE_SULFO < 0 ? 1E-12 : C_TOT_BILE_SULFO);

        C_BRAIN              = (C_BRAIN          < 0 ? 1E-10 : C_BRAIN);
        C_GONADS   = (C_GONADS                  < 0 ? 1E-10 : C_GONADS);
        C_PP                 = (C_PP                    < 0 ? 1E-10 : C_PP);

        C_ART                = (C_ART           < 0 ? 1E-10 : C_ART);
        C_LIVER              = (C_LIVER         < 0 ? 1E-10 : C_LIVER);
        C_CARCASS  = (C_CARCASS         < 0 ? 1E-10 : C_CARCASS);

        C_ART_GLUCO                     = (C_ART_GLUCO      < 0 ? 1E-10 : C_ART_GLUCO);
        C_LIVER_GLUCO        = (C_LIVER_GLUCO< 0 ? 1E-10 : C_LIVER_GLUCO);
        C_ROB_GLUCO                     = (C_ROB_GLUCO      < 0 ? 1E-10 : C_ROB_GLUCO);

        C_ART_SULFO                     = (C_ART_SULFO      < 0 ? 1E-10 : C_ART_SULFO);
        C_LIVER_SULFO        = (C_LIVER_SULFO< 0 ? 1E-10 : C_LIVER_SULFO);
        C_ROB_SULFO                     = (C_ROB_SULFO      < 0 ? 1E-10 : C_ROB_SULFO);

        #NEEDED TO CALIBRATE EXCRETION IN LINDHOLST 2003
        C_TOT_PC =  (C_TOT_LIND >1E-12 ? C_TOT_BILE/ C_TOT_LIND : 1E-12);
        C_TOT_GLUCO_PC = (C_TOT_GLUCO_LIND >1E-12 ? C_TOT_BILE_GLUCO/ C_TOT_GLUCO_LIND : 1E-12);
        C_TOT_SULFO_PC = (C_TOT_SULFO_LIND >1E-12 ? C_TOT_BILE_SULFO/ C_TOT_SULFO_LIND : 1E-12);
```

```
    # MASS-BALANCE

          LENGTH =  L/DEB_SHAPE ; # PHYSICAL LENGTH (MM)
          Q_BODY                          = (Q_ART + Q_VEN + Q_LIVER + Q_GONADS + Q_BRAIN + Q_FAT + Q_SKIN + Q_KIDNEY + Q_VISCERA +
Q_PP + Q_RP );

          Q_ADMIN_TOT                     = Q_ADMIN_GILLS + IVQUANTITY ; # AMOUNT ENTERING BODY

          Q_ELIM_TOT           = Q_EXCRET + Q_MET;

          MASS_BAL             = Q_ADMIN_TOT - Q_BODY - Q_ELIM_TOT ;
          # MASS_BAL_SYS       = (Q_ADMIN_TOT - Q_ADMIN_GILLS) - Q_BODY - ( Q_ELIM_TOT - Q_EXCRET) - Q_WATER ;

          MASS_BAL_GLUCO       =         (Q_MET_PLASMA_GLUCO        +        Q_MET_LIVER_GLUCO)        *        CONV_GLUCO        -
(Q_LIVER_GLUCO+Q_ROB_GLUCO+Q_ART_GLUCO+Q_VEN_GLUCO  +  Q_LUMEN_GIT_GLUCO  +  Q_BILE_GLUCO  +  Q_GONADS_GLUCO  +  Q_ABDO_CAVITY_GLUCO)  -
Q_EXCRET_GLUCO ;
          MASS_BAL_SULFO       =         (Q_MET_LIVER_SULFO        +        Q_MET_PLASMA_SULFO)        *        CONV_SULFO        -
(Q_LIVER_SULFO+Q_ROB_SULFO+Q_ART_SULFO+Q_VEN_SULFO  +  Q_LUMEN_GIT_SULFO  +  Q_BILE_SULFO  +  Q_GONADS_SULFO  +  Q_ABDO_CAVITY_SULFO)  -
Q_EXCRET_SULFO ;

          C_BISPHENOL          = (C_TOT_BILE + C_TOT_BILE_GLUCO + C_TOT_BILE_SULFO);


    #TRANSFORMATION FOR CALIBRATION

          RATIO_PHAGO_PERCENT = RESPONSE_PHAGO_PERCENT/R0_PHAGO ;
          RATIO_TBARS = RESPONSE_TBARS/R0_TBARS ;
          RATIO_ROSA = RESPONSE_ROSA/R0_ROSA ;
          RATIO_MACRO_PERCENT = RESPONSE_MACRO_PERCENT/R0_MACRO ;
          RATIO_LYSO = RESPONSE_LYSO/R0_LYSO;
          RATIO_PHAGO_PERCENT  = (RATIO_PHAGO_PERCENT< 0 ? 1E-10 : RATIO_PHAGO_PERCENT);
          RATIO_TBARS                     = (RATIO_TBARS       < 0 ? 1E-10 : RATIO_TBARS);
          RATIO_ROSA = (RATIO_ROSA< 0 ? 1E-10 : RATIO_ROSA);
          RATIO_MACRO_PERCENT             = (RATIO_MACRO_PERCENT         < 0 ? 1E-10 : RATIO_MACRO_PERCENT);

          RATIO_LYSO = (RATIO_LYSO< 0 ? 1E-10 : RATIO_LYSO);

    } # END OF CALCOUTPUTS

    END.
```

7.2. MCsim input files:

```
    ### MCMC
    ### SUBSTANCE : BPA
    ### BIOMARKERS : PHAGOCYTOSIS (EFFICIENCY) - GRANULOCYTE-MACROPHAGE - LYSOSOMAL PRESENCE - TBARS

    ### UNITS:
    # QUANTITY          MICROG
    # VOLUMES:          ML
    # TIME:             D
    # FLOWS:            ML/D
    # CONCENTRATIONS:   MICROG/ML
    # VMAX:             MICROG/D/ ML LIVER
    # KM:               MICROG/ML
    # MASSES:           G
    # LENGHT:           MM
    # TEMPERATURE:      CELSIUS
    # VENTILATION RATE: ML/D

    # AUTHORS : CORENTIN MIT
    # DATE : 06/2022
    #_PHYSIOLOGICAL VLAUES : MALE
    #================================================

    INTEGRATE( LSODES, 1E-8, 1E-10, 1);

    SETPOINTS("PHAGOCYTOSIS_BPA.OUT", "TAB_SETPOINT.OUT", 0 ,
                            K_TOL_PHAGO, S_MAX_PHAGO, SC_50_PHAGO, KR_DELAY, TAU, SIGMA_C_PHAGO);



          K_IN_PHAGO = 978.69;
          K_OUT_PHAGO = 37.42;
          R0_PHAGO = 26.15 ;

          #A PRIORI PARAMETER DISTRIBUTIONS
          UNBOUND_FRACTION = 0.067;
          UNBOUND_FRACTION_GLUCO = 0.95  ;          # BETWEEN 0 AND 1
          UNBOUND_FRACTION_SULFO = 0.95  ;          # BETWEEN 0 AND 1

          # KM EST EN µMOL/ML ET VMAX EN µG/JOUR/G DE FOIE
          KM_GLUCO = 40.0;
          KM_SULFO = 7.6;
          RATIO_VMAX_KM_GLUCO = 10.0;
          RATIO_VMAX_KM_SULFO = 1.5;

          CL_PLASMA_GLUCO = 38648.1;
          CL_PLASMA_SULFO = 375.7;


          RATIO_PC_UF = 4.4;
          PC_LIVER = 4.8;
          PC_GONADS = 5.6;
          PC_VISCERA           = 1.1     ;          # PARTITION COEF VISCERA FOR BPA
          PC_FAT = 0.63;
```

```
PC_KIDNEY            = 4.3     ;          # Partition coef kidney  for BPA
PC_SKIN                        = 1.2     ;          # Partition coef skin  for BPA
PC_BRAIN             = 1.9     ;          # Partition coef skin  for BPA
PC_RP = 0.18;
PC_PP = 0.53;


PC_LIVER_GLUCO = 3.3;
PC_ROB_GLUCO = 0.14;
PC_ABDO_CAVITY_GLUCO = 6.89;
PC_GONADS_GLUCO                        = 6.92;
KE_BILE_GLUCO = 94.3;

PC_LIVER_SULFO = 3.7;
PC_ROB_SULFO = 0.31;
PC_ABDO_CAVITY_SULFO = 7.46;
PC_GONADS_SULFO                        = 7.28;
KE_BILE_SULFO = 62.8;

K_BG      = 1E10    ; # Excreted flow from billiary vesicule to faeces (1/d)
KE_BILE   = 1E-12   ; # Excreted flow of BPA from liver to billiary vesicule (1/d)

Abs_eff =1.0;
PLASMA = 0.55 ; # Stickleback https://doi.org/10.1242/jeb.065425

#Phago
S_MAX_PHAGO =1.0 ;#Distrib(S_MAX_PHAGO, TruncNormal_cv, 1.8, 0.3, 1E-3, 1E3);
SC_50_PHAGO =1.0;#Distrib(SC_50_PHAGO, TruncNormal_cv, 0.2, 0.3, 1E-3, 1E3);
K_TOL_PHAGO =1.0;#Distrib(K_TOL_PHAGO, TruncNormal_cv, 0.1, 0.3, 1E-6, 10.0);
KR_DELAY =1.0; #Distrib(KR_DELAY, TruncNormal_cv, 1.0, 0.3, 1E-4, 100.0);
TAU = 1.0; #Distrib(TAU,  TruncNormal_cv, 8.0, 0.3, 7.0, 13.0);

#ROS A
R0_ROSA = 1.0;# Distrib(R0_PHAGO, TruncNormal_cv, 27.0, 0.3, 1E-4, 100.0);#Marchand et al., 2018
K_OUT_ROSA = 1.0;# Distrib(K_OUT_PHAGO,  Uniform, 1E-6, 1E6);
S_MAX_ROSA = 1.0;# Distrib(S_MAX_PHAGO, TruncNormal_cv, 1.8, 0.3, 1E-3, 1E3);
SC_50_ROSA = 1.0;# Distrib(SC_50_PHAGO, TruncNormal_cv, 0.2, 0.3, 1E-3, 1E3);
SIGMA_C_ROSA = 1.0;# Distrib(SIGMA_C_PHAGO, HalfNormal, 2);

# # Macrophages
R0_MACRO = 1.0 ;# Distrib(R0_MACRO, TruncNormal_cv, 35.0, 0.3, 1E-4, 100.0);#Marchand et al., 2018
K_OUT_MACRO = 1.0 ;# Distrib(K_OUT_MACRO,  Uniform, 1E-6, 1E6);
EC_50_MACRO= 1.0 ;# Distrib(EC_50_MACRO, TruncNormal_cv, 0.2, 0.3, 1E-3, 1E3);
SIGMA_C_MACRO = 1.0;# Distrib(SIGMA_C_MACRO, HalfNormal, 2);

# #TBARS
R0_TBARS= 1.0;# Distrib(R0_TBARS, TruncNormal_cv, 27.0, 0.3, 1E-4, 100.0);#Marchand et al., 2018
K_OUT_TBARS= 1.0;# Distrib(K_OUT_TBARS,  Uniform, 1E-6, 1E6);
S_MAX_TBARS= 1.0;# Distrib(S_MAX_TBARS, TruncNormal_cv, 1.8, 0.3, 1E-3, 1E3);
SC_50_TBARS= 1.0;# Distrib(SC_50_TBARS, TruncNormal_cv, 0.2, 0.3, 1E-3, 1E3);


# #Lysosomes
R0_LYSO= 1.0;# Distrib(R0_LYSO, TruncNormal_cv, 200.0, 0.3, 10, 1E4);#Marchand et al., 2018
K_OUT_LYSO= 1.0;# Distrib(K_OUT_LYSO,  Uniform, 1E-6, 1E6);
S_MAX_LYSO= 1.0;# Distrib(S_MAX_LYSO, TruncNormal_cv, 1.8, 0.3, 1E-3, 1E3);
SC_50_LYSO= 1.0;# Distrib(SC_50_LYSO, TruncNormal_cv, 0.2, 0.3, 1E-3, 1E3);
SIGMA_C_LYSO= 1.0;# Distrib(SIGMA_C_LYSO, HalfNormal, 2);


Simulation { #Stickleback(control) # seven-day exposure

        # Physiological parameters
        BW_FCARD_REF= 0.294  ;  # Body weight of reference for F_CARD from Ekstrom, 2016 (Perch value)
        BW_VO2_REF = 0.97    ;  # Body weight of reference for VO2 from Brafield, 1976 and Walkey, 1970
        DEB_V      = 1.26    ;  # Energy conductance (mm/d) (DEB model parameter)
        DEB_G      = 0.7398  ;  # Energy investment ratio (SU) (DEB model parameter)
        DEB_KM     = 0.122   ;  # Somatic maintenance rate coefficient (1/d) (DEB model parameter)
        DEB_EHM    = 1       ;  # Energy at State of maturity at metamorphosis (J)
        DEB_EHB    = 1       ;  # Energy at State of maturity at birth (J)
        DEB_SHAPE  = 0.247   ;
        A_BW_L     = 0.01543825; # = (0.249^3),  # Bw= a*TL^b parameter  (mg/mm)
        B_BW_L     = 3.0     ;  # b relation BW(mg)=F(L(mm)) --> SU

        # Environmental condition
        TA           = 6130 ;    # Arrhenius temperature  in Kelvin
        TR_DEB       = 293.65;   # (Kelvin)
        TR_FCARD     = 289.15;   # (Kelvin) -> temperature oprimal : 16 C
        TR_VO2       = 283.15;   # (Kelvin)
        TR_EXCRETION = 289.15;   # (Kelvin)

        # Effective respiratory volume & cardiac output
        F_CARD_REF  = 62.96969        ;  #  =  QB_REF_PERCH  *  (BW_REF^(0.75))  /  BW_REF  #  (ML/D/G)  =  46.368  *
(0.294^(0.75)) / 0.294 --> allometric scalling function from Ekstrom,2016
        V_O2_REF    = 4.03            ; # reference oxygen comsuption rate (mg O2/g/d) --> from Brafield, 1976
        O2_EE       = 0.71            ; # Oxygen extraction efficiency of 71% proposed by Erickson, 1990
        SAT         = 0.90            ; # dissolved oxygen saturation of 90% proposed by Erickson, 1990

        # volume scaling factor : fraction of BW (%)
        SC_BLOOD  = 0.009 ;
        SC_GONADS = 0.00781598 ;
        SC_BRAIN  = 0.012 ;
        SC_LIVER  = 0.053860073 ;
        SC_FAT    = 0.0168;
        SC_SKIN   = 0.036 ;
        SC_VISCERA= 0.055 ;
        SC_KIDNEY = 0.011725124 ;
        SC_RP     = 0.032 ;

        # Fraction of arterial blood flow
        FRAC_GONADS =0.0054 ;
        FRAC_BRAIN  =0.0392 ;
        FRAC_LIVER  =0.0529 ;
```

```
                FRAC_FAT    =0.0095 ;
                FRAC_SKIN   =0.0186 ;
                FRAC_VISCERA=0.0886 ;
                FRAC_KIDNEY =0.114 ;
                FRAC_RP     =0.1074 ;

                #INPUTS
                BW_I                = 1.53; #MEAN MASS OF FISH
                TEMPERATURE         = 16;
                F_CST               = 0.82;
                V_WATER             = 1E+12 ;#ML
                IVQUANTITY = 0.0;
                EVENT_BILE = 1;

                C_WATER= 0.0;

                #EXPERIMENTAL DATA
                PRINTSTEP(RESPONSE_PHAGO_PERCENT,  0, 14, 0.05);

                PRINTSTEP(RESPONSE_PHAGO_PERCENT,  0, 14, 0.05);
                PRINTSTEP(RATIO_PHAGO_PERCENT,  0, 14, 0.05);
                PRINTSTEP(C_RP, 0, 14, 0.05);
        }

        SIMULATION { #STICKLEBACK AT 10 µG/L (NOMINAL CONCENTRATION) # SEVEN-DAY EXPOSURE

                # PHYSIOLOGICAL PARAMETERS
                BW_FCARD_REF= 0.294  ;  # BODY WEIGHT OF REFERENCE FOR F_CARD FROM EKSTROM, 2016 (PERCH VALUE)
                BW_VO2_REF = 0.97    ;  # BODY WEIGHT OF REFERENCE FOR VO2 FROM BRAFIELD, 1976 AND WALKEY, 1970
                DEB_V      = 1.26    ;  # ENERGY CONDUCTANCE (MM/D) (DEB MODEL PARAMETER)
                DEB_G      = 0.7398  ;  # ENERGY INVESTMENT RATIO (SU) (DEB MODEL PARAMETER)
                DEB_KM     = 0.122   ;  # SOMATIC MAINTENANCE RATE COEFFICIENT (1/D) (DEB MODEL PARAMETER)
                DEB_EHM    = 1       ;  # ENERGY AT STATE OF MATURITY AT METAMORPHOSIS (J)
                DEB_EHB    = 1       ;  # ENERGY AT STATE OF MATURITY AT BIRTH (J)
                DEB_SHAPE  = 0.247   ;
                A_BW_L     = 0.01543825; # = (0.249^3),  # BW= A*TL^B PARAMETER  (MG/MM)
                B_BW_L     = 3.0     ;  # B RELATION BW(MG)=F(L(MM)) --> SU

                # ENVIRONMENTAL CONDITION
                TA          = 6130 ;    # ARRHENIUS TEMPERATURE  IN KELVIN
                TR_DEB       = 293.65;   # (KELVIN)
                TR_FCARD     = 289.15;   # (KELVIN) -> TEMPERATURE OPRIMAL : 16 C
                TR_VO2       = 283.15;   # (KELVIN)
                TR_EXCRETION = 289.15;   # (KELVIN)

                # EFFECTIVE RESPIRATORY VOLUME & CARDIAC OUTPUT
                F_CARD_REF  = 62.96969        ;  #  =  QB_REF_PERCH  *  (BW_REF^(0.75))  /  BW_REF  #  (ML/D/G)  =  46.368  *
(0.294^(0.75)) / 0.294 --> ALLOMETRIC SCALLING FUNCTION FROM EKSTROM,2016
                V_O2_REF    = 4.03            ; # REFERENCE OXYGEN COMSUPTION RATE (MG O2/G/D) --> FROM BRAFIELD, 1976
                O2_EE       = 0.71            ; # OXYGEN EXTRACTION EFFICIENCY OF 71% PROPOSED BY ERICKSON, 1990
                SAT         = 0.90            ; # DISSOLVED OXYGEN SATURATION OF 90% PROPOSED BY ERICKSON, 1990

                # VOLUME SCALING FACTOR : FRACTION OF BW (%)
                SC_BLOOD  = 0.009 ;
                SC_GONADS = 0.00781598 ;
                SC_BRAIN  = 0.012 ;
                SC_LIVER  = 0.053860073 ;
                SC_FAT    = 0.0168;
                SC_SKIN   = 0.036 ;
                SC_VISCERA= 0.055 ;
                SC_KIDNEY = 0.011725124 ;
                SC_RP     = 0.032 ;

                # FRACTION OF ARTERIAL BLOOD FLOW
                FRAC_GONADS =0.0054 ;
                FRAC_BRAIN  =0.0392 ;
                FRAC_LIVER  =0.0529 ;
                FRAC_FAT    =0.0095 ;
                FRAC_SKIN   =0.0186 ;
                FRAC_VISCERA=0.0886 ;
                FRAC_KIDNEY =0.114 ;
                FRAC_RP     =0.1074 ;

                #INPUTS
                BW_I                = 1.67; #MEAN MASS OF FISH
                TEMPERATURE         = 16;
                F_CST               = 0.82;
                V_WATER             = 1E+12 ;#ML
                IVQUANTITY = 0.0;
                EVENT_BILE = 1;

      C_WATER= NDOSES( 171 ,

         0.00025,0.000849747474747475,0.00144949494949495,0.00204924242424242,0.0026489898989899,0.00324873737373737,
0.00384848484848485,0.00444823232323232,0.00500099502487562,0.0050134328358209,0.00502587064676617,0.0050383084577114
4,0.00505074626865672,0.00506318407960199,0.00507562189054726,0.00508805970149254,0.00510049751243781,0.0051129353233
8308,0.00512537313432836,0.00513781094527363,0.00515024875621891,0.00516268656716418,0.00517512437810945,0.0051875621
8905473,0.0052,0.00522083333333333,0.00524166666666667,0.0052625,0.00528333333333333,0.00530416666666667,0.005325,0.0
0534583333333333,0.00536666666666667,0.0053875,0.00540833333333333,0.00542916666666667,0.00545,0.00547083333333333,0.
00549166666666667,0.0055125,0.00553333333333333,0.00555416666666667,0.005575,0.00559583333333333,0.00561666666666667,
0.0056375,0.00565833333333333,0.00567916666666667,0.0057,0.00570208333333333,0.00570416666666667,0.00570625,0.0057083
3333333333,0.00571041666666667,0.0057125,0.00571458333333333,0.00571666666666667,0.00571875,0.00572083333333333,0.005
72291666666667,0.005725,0.00572708333333333,0.00572916666666667,0.00573125,0.00573333333333333,0.00573541666666667,0.
0057375,0.00573958333333333,0.00574166666666667,0.00574375,0.00574583333333333,0.00574791666666667,0.00575,0.00575208
333333333,0.00575416666666667,0.00575625,0.00575833333333333,0.00576041666666667,0.0057625,0.00576458333333333,0.00577
6666666666667,0.00576875,0.00577083333333333,0.00577291666666667,0.005775,0.00577708333333333,0.00577916666666667,0.0
0578125,0.00578333333333333,0.00578541666666667,0.0057875,0.00578958333333333,0.00579166666666667,0.00579375,0.005795
83333333333,0.00579791666666667,0.0058,0.00578125,0.0057625,0.00574375,0.005725,0.00570625,0.0056875,0.00566875,0.005
65,0.00563125,0.0056125,0.00559375,0.005575,0.00555625,0.0055375,0.00551875,0.0055,0.00548125,0.0054625,0.00544375,0.
005425,0.00540625,0.0053875,0.00536875,0.00535,0.00533125,0.0053125,0.00529375,0.005275,0.00525625,0.0052375,0.005218
75,0.0052,0.00518125,0.0051625,0.00514375,0.005125,0.00510625,0.0050875,0.00506875,0.00505,0.00503125,0.0050125,0.004
99375,0.004975,0.00495625,0.0049375,0.00491875,0.0049,0.0049,0.0049,0.0049,0.0049,0.0049,0.0049,0.0049,0.0049,
```

```
0.0049,0.0049,0.0049,0.0049,0.0049,0.0049,0.0049,0.0049,0.0049,0.0049,0.0049,0.0049,0.0049,0.0049,0.0049,0.000
25 ,

         0,0.0416666666666667,0.0833333333333333,0.125,0.166666666666667,0.208333333333333,0.25,0.291666666666667,0.3
33333333333333,0.375,0.416666666666667,0.458333333333333,0.5,0.541666666666667,0.583333333333333,0.625,0.666666666666
667,0.708333333333333,0.75,0.791666666666667,0.833333333333333,0.875,0.916666666666667,0.958333333333333,1,1.04166666
666667,1.08333333333333,1.125,1.16666666666667,1.20833333333333,1.25,1.29166666666667,1.33333333333333,1.375,1.41666
66666667,1.45833333333333,1.5,1.54166666666667,1.58333333333333,1.625,1.66666666666667,1.70833333333333,1.75,1.79166
66666667,1.83333333333333,1.875,1.91666666666667,1.95833333333333,2,2.04166666666667,2.08333333333333,2.125,2.16666666
6666667,2.20833333333333,2.25,2.29166666666667,2.33333333333333,2.375,2.41666666666667,2.45833333333333,2.5,2.5416666
6666667,2.58333333333333,2.625,2.66666666666667,2.70833333333333,2.75,2.79166666666667,2.83333333333333,2.875,2.91666
666666667,2.95833333333333,3,3.04166666666667,3.08333333333333,3.125,3.16666666666667,3.20833333333333,3.25,3.2916666
6666667,3.33333333333333,3.375,3.41666666666667,3.45833333333333,3.5,3.54166666666667,3.58333333333333,3.625,3.666666
66666667,3.70833333333333,3.75,3.79166666666667,3.83333333333333,3.875,3.91666666666667,3.95833333333333,4,4.04166666
666667,4.08333333333333,4.125,4.16666666666667,4.20833333333333,4.25,4.29166666666667,4.33333333333333,4.375,4.416666
66666667,4.45833333333333,4.5,4.54166666666667,4.58333333333333,4.625,4.66666666666667,4.70833333333333,4.75,4.791666
66666667,4.83333333333333,4.875,4.91666666666667,4.95833333333333,5,5.04166666666667,5.08333333333333,5.125,5.1666666
6666667,5.20833333333333,5.25,5.29166666666667,5.33333333333333,5.375,5.41666666666667,5.45833333333333,5.5,5.5416666
6666667,5.58333333333333,5.625,5.66666666666667,5.70833333333333,5.75,5.79166666666667,5.83333333333333,5.875,5.91666
666666667,5.95833333333333,6,6.04166666666667,6.08333333333333,6.125,6.16666666666667,6.20833333333333,6.25,6.2916666
6666667,6.33333333333333,6.375,6.41666666666667,6.45833333333333,6.5,6.54166666666667,6.58333333333333,6.625,6.666666
66666667,6.70833333333333,6.75,6.79166666666667,6.83333333333333,6.875,6.91666666666667,6.95833333333333,7,7.04166666
666667,7.08333333333333 );


                #EXPERIMENTAL DATA
                PRINTSTEP(RESPONSE_PHAGO_PERCENT,  0, 14, 0.05);
                PRINTSTEP(RATIO_PHAGO_PERCENT,  0, 14, 0.05);
                PRINTSTEP(C_RP, 0, 14, 0.05);
        }

    END.
```

7.3. **tab_setpoint.out**

```
    K_TOL_PHAGO.1. S_MAX_PHAGO.1. SC_50_PHAGO.1. KR_DELAY.1. TAU.1. SIGMA_C_PHAGO.1.
      0.980969 0.215426 0.127866 0.841498 12.1557 1.10211
     0.980969 0.362681 0.127866 0.841498 11.7805 1.10211
     0.74399 0.362681 0.127866 0.841498 11.7805 1.11414
     0.670547 0.362681 0.099472 1.29955 11.7805 1.11137
     0.552054 0.269903 0.088233 1.29955 11.7805 1.11736
     0.566126 0.358806 0.088233 1.29955 10.7693 1.10922
     0.566126 0.327516 0.088233 1.29955 12.3661 1.11079
     0.64649 0.1897 0.0648158 1.29955 12.9026 1.10179
     0.480384 0.252511 0.0550445 1.29955 12.9573 1.10519
     0.480384 0.252511 0.126588 1.29955 10.0259 1.10519
     0.248284 0.252511 0.0516114 1.29955 10.0259 1.11711
     0.248284 0.252511 0.0516114 1.29955 10.0259 1.1144
     0.369525 0.252511 0.0528741 1.29955 9.7715 1.1144
     0.369525 0.252511 0.0528741 1.29955 9.7715 1.11075
     0.369525 0.21298 0.0828182 1.29955 9.7715 1.11075
     0.243819 0.21298 0.0828182 1.29955 9.7715 1.11711
     0.243819 0.254703 0.0828182 1.29955 9.7715 1.11711
     0.243819 0.254703 0.0828182 1.29955 9.7715 1.1109
     0.286479 0.285945 0.0828182 1.29955 9.7715 1.10491
     0.520976 0.285945 0.0828182 1.29955 11.4773 1.11723
     0.521397 0.254066 0.0828182 1.29955 11.4773 1.10544
     0.563571 0.254066 0.0828182 1.29955 11.4773 1.10544
     0.626506 0.254066 0.0828182 1.29955 11.4773 1.11938
     0.776005 0.254066 0.0974643 1.29955 11.4773 1.11226
     0.776005 0.254066 0.0974643 1.10119 11.4773 1.10348
     0.698628 0.254066 0.0974643 1.10119 11.4773 1.10348
     0.495041 0.254066 0.1197 1.10119 11.4773 1.10726
     0.548764 0.254066 0.1197 1.10119 11.4773 1.10476
     0.556748 0.339658 0.0940046 1.10119 10.1922 1.10476
     0.556748 0.274329 0.0940046 1.10119 10.1922 1.10202
     0.765615 0.25802 0.0940046 1.19235 10.1922 1.11361
     0.767867 0.25802 0.0940046 1.24257 10.1922 1.11361
     0.682536 0.25802 0.0443906 1.24257 10.1922 1.11361
     0.776613 0.25802 0.0443906 1.24257 10.1922 1.11361
    MVP 0.860222 0.276636 0.0983165 1.00413 12.3328 1.10006
```

8. References

Bado-Nilles, A., S. Betoulle, A. Geffard, J.-M. Porcher, B. Gagnaire, and W. Sanchez. 2013. Flow cytometry detection of lysosomal presence and lysosomal membrane integrity in the three-spined stickleback (Gasterosteus aculeatus L.) immune cells: applications in environmental aquatic immunotoxicology. Environmental Science and Pollution Research **20**:2692-2704.

Bado-Nilles, A., R. Techer, J. M. Porcher, A. Geffard, B. Gagnaire, S. Betoulle, and W. Sanchez. 2014. Detection of immunotoxic effects of estrogenic and androgenic endocrine disrupting compounds using splenic immune cells of the female three-spined stickleback, Gasterosteus aculeatus (L.). Environmental Toxicology and Pharmacology **38**:672-683.

Bois, F. Y. 2009. GNU MCSim: Bayesian statistical inference for SBML-coded systems biology models. Bioinformatics **25**:1453-1454.

Gagnaire, B., H. Thomas-Guyon, and T. Renault. 2004. In vitro effects of cadmium and mercury on Pacific oyster, Crassostrea gigas (Thunberg), haemocytes. Fish & Shellfish Immunology **16**:501-512.

R Core Team. 2019. R: A Language and Environment for Statistical Computing. R Foundation for Statistical Computing, Vienna, Austria.